Intelligent Geoengineering 3 (2026) 36–56

Contents lists available at ScienceDirect

Intelligent Geoengineering

journal homepage: www.keaipublishing.com/en/journals/ige/

Full length article

Quantitative morphological analysis of rock particles on laser scanner data using deep learning

Mojgan Faramarzi. H, Kamran Esmaeili*

Department of Civil & Mineral Engineering, University of Toronto, Toronto M5S2E8, Canada

ARTICLE INFO

Keywords:
Particle shape analysis
3D Morphology
Point cloud segmentation
Synthetic data generation
Computer vision
Deep learning

ABSTRACT

While size distribution has traditionally been the dominant metric in rock fragmentation, studies have shown that both size and shape characteristics are influential in determining energy consumption, equipment wear, flowability, and efficiency. The main objective of this research is to provide a scalable, quantitative, and light-independent method for characterizing the 3D shape of rock fragments. This work leverages an existing deep learning approach that combines LiDAR-based point cloud acquisition with deep learning instance segmentation. Trained on a synthetic 3D labeled dataset, the deep learning model, SoftRock, accurately segments individual rock pieces and provides key shape metrics such as sphericity, angularity, aspect ratio, and longest dimension for each rock in the pile. The model's performance was then validated on three distinct rock piles curated to represent different spectrum of rock types and sizes, including blasted limestone from a quarry, rounded pebbles, and crushed copper ore from a conveyor belt. The model demonstrated a high level of accuracy across these diverse samples, with the error for key shape metrics ranging from 2% to 16%. While some inaccuracies were observed, primarily due to the sensitivity of sphericity and angularity to noise in the point cloud data, our findings validate the model's ability to capture key shape characteristics. This study provides a foundational framework for integrating comprehensive 3D particle morphology into mining workflows, offering more accurate data to inform decisions that enhance operational efficiency and equipment longevity.

1. Introduction

Assessing material properties and characteristics promptly after blasting, whether in open-pit or underground mining operations, remains a major operational concern. These evaluations have a direct impact on operational efficiency, cost reduction. While particle size distribution has long been central to fragmentation research, understanding particle shape provides deeper insights into flowability, energy consumption, and equipment wear, contributing to more informed decision-making and improved performance across mining operations. Fig. 1 presents two different rockpiles with distinct shapes, one consisting of more angular particles and the other of more rounded ones.

Studies on rock characteristics emphasize both size and shape as critical factors that affect operational performance, lower energy demands, and support more efficient equipment maintenance (Li et al., 2021; Ouchterlony, 2003; Taylor, 2002; Wills and Finch, 2015). Current research on particle shape evaluation has primarily focused on particles in geology and sedimentology, rockfill materials, asphalt concrete aggregates, and tailings (Li et al., 2021). As noted by Li et al. (2023), “The existing methods can only characterize the shape features of particles within a certain particle size range, whereas the particle size and shape of blasting fragments vary widely, posing challenges to the characterization of their shape properties.” Shape analysis is a crucial complement to size distribution analysis in mining that offers essential insights to support operational optimization and cost reduction. While size distribution provides a measure of particle dimensions, shape characteristics such as sphericity, angularity, longest dimension, and elongation aspect ratio reveal deeper aspects of particle behavior, particularly in material handling and processing. As described by Ouchterlony (2003), “fragmentation can be characterized in terms of a fragment size distribution and the shape and angularity or roundness of the fragments, i.e., essentially geometrical data.”

Peer review under responsibility of Chinese Society for Rock Mechanics and Engineering
* Correspondence author at: University of Toronto, Toronto M5S2E8, Canada.
E-mail addresses: mozhgan.faramarzi@mail.utoronto.ca (M. Faramarzi. H), kamran.esmaeili@utoronto.ca (K. Esmaeili).

https://doi.org/10.1016/j.ige.2026.04.002
Received 30 September 2025; Received in revised form 23 February 2026; Accepted 8 April 2026
Available online 9 April 2026

Fig. 1. Sample rockpiles with different shapes, left: more angular particles, right: more rounded particles.

Particle interlocking and blockages are significant challenges in material handling within underground mining operations, particularly in ore passes and drawpoints in block cave mines. Irregularly shaped particles can hinder material flow, leading to operational delays, safety risks, and inefficiencies (Wang et al., 2022).

Shape analysis provides insights into interlocking mechanisms and flow behavior which enables development of strategies to minimize blockages and enhance the performance of material handling and transport systems. Similarly, conveyor belts, chute systems, shovel nails, and grinding liners often experience wear and segregation due to irregularities in particle shape, which increases maintenance requirements and operational costs. Moreover, shape analysis plays a crucial role in downstream processes such as crushing, grinding, and screening. Angular or elongated particles often behave differently during grinding than more spherical particles, affecting energy consumption and the uniformity of the final product size (Cleary and Owen, 2019). In screening operations, irregular particle shapes can hinder accurate classification, reducing the efficiency of mineral recovery processes. Additionally, in flotation and other separation techniques, the surface area-to-volume ratios influenced by particle shape directly impact reagent interaction and recovery rates (Koh et al., 2009). Beyond processing operations, the shape of rock particles plays a crucial role in determining the structural stability of waste piles and embankments. The interlocking and packing behavior of irregular particles can significantly influence settlement patterns and slope stability of the piles (Zardari, 2011). This understanding helps prevent slope failures and mitigate environmental risks. Therefore, there is a significant untapped potential to extend these shape analysis techniques to rock fragmentation and benefit from them in mining.

1.1. Application of particle shape analysis in mining and mineral processing

Particle shape analysis offers critical insights into rock fragment behavior, impacting key processes such as transport, crushing, grinding, screening, and flotation. Understanding characteristics like angularity, roundness, and aspect ratio helps improve operational efficiency, reduce energy consumption, and extend equipment longevity. Despite widespread recognition of shape's importance, quantitative integration of shape metrics into predictive operational models remains a significant research challenge.

Particle shape, particularly angularity, plays a key role in material flow within mining operations (Ali et al., 2023; Xia, 2017; Firouzabadi et al., 2023). Angular particles tend to interlock, reducing flowability in chutes, hoppers, conveyors, and ore passes. This interlocking behavior leads to blockages, uneven transport, and inaccurate size distribution due to excessive pile-up. In contrast, rounder particles move more freely, enabling smoother flow, reduced downtime, and lower energy use (Wang et al., 2022). Additionally, particle shape impacts the energy required for loading and hauling. Angular particles result in higher energy consumption, as they resist movement due to their interlocking nature. This not only increases the fuel consumption of loading machinery but also reduces productivity due to the difficulty in loading and hauling. Particles with high aspect ratios (elongated shapes) exhibit different flow behavior, packing density, and interlock properties compared to near-spherical particles of equal volume. Size distribution alone cannot predict bridging in bins, chute blockages, or transport belt surging; operational disruptions that shape analysis can anticipate.

Sharp, angular fragments are more abrasive, accelerating wear on shovels, belts, and handling systems. This raises maintenance costs and shortens equipment lifespan. Understanding particle shape enables the forecasting of wear, proactive scheduling of maintenance, and the selection of better-suited materials for wear-prone components. Moreover, particle shape influences the stability of blasted rock piles. Angular particles interlock more efficiently, creating more stable rock piles (e.g. waste rock dumps). This is critical for safety, as unstable piles can lead to failure, endangering workers and equipment. Shape analysis aids in modeling pile behavior and designing safer mine layouts and minimizing the risks of failure.

Understanding the morphological characteristics of rock particles is essential for effective mineral processing as well. Crushing and grinding (comminution) are energy-intensive processes. Angular particles resist breakage due to their interlocking nature and require more energy to process, whereas round particles fracture more easily, thereby reducing energy use. Shape analysis helps optimize the grinding process, improving energy efficiency and reducing operational costs (Pereira et al., 2023; Danjo et al., 1989; Elmsahli and Sinka, 2021). Gan et al. (2019) quantified that specific breakage energy varies as a function of both size and sphericity ($e_m = k_1 \cdot d^{-0.5} \cdot \psi^{k_2}$, where e_m is specific breakage energy (J/kg), d is particle size, ψ is sphericity, and k_1, k_2 are material-dependent coefficients), meaning two particles of identical mass but different sphericity require different grinding energies. For magnetite ore, their experiments showed sphericity variations from 0.5 to 0.9 corresponded to measurable changes in breakage energy at constant size, demonstrating that size-only predictions systematically misestimate energy requirements when shape distributions vary between blast patterns or ore sources.

The particle shape can significantly impact the efficiency of separation processes as well. In flotation, particle shape affects reagent interaction and recovery. Angular particles often have larger surface areas, which improves recovery rates for valuable minerals such as gold and chalcopyrite (Wills and Napier-munn, 2006).

Similar to mining, angular particles accelerate wear in processing equipment such as crushers, mills, and conveyor belts. Ou and Chen (2023) documented that angular particles cause substantially higher

crusher liner wear compared to rounded particles, though the relationship remains difficult to quantify. Two fragmentation events producing identical P80 values but different angularity distributions will induce dramatically different maintenance requirements; information invisible to size-only monitoring. Shape analysis enables more accurate wear prediction and proactive maintenance, thereby minimizing downtime. This leads to cost savings and improved equipment longevity, ensuring that the plant operates at peak efficiency (Tang et al., 2021).

The recurring theme across mining and mineral processing applications is that while shape's qualitative importance is universally acknowledged and extensively documented, quantitative integration into operational predictive models remains largely unrealized. The literature remains dominated by qualitative observations rather than validated predictive equations. Researchers consistently report that "angular particles cause higher wear", that "shape affects flotation", and that "angularity reduces flowability", yet these insights have not been translated into operational models with explicit shape parameters analogous to how particle size appears in variety of formulas. The relationships are widely experienced and observed but not mathematically formalized for predictive use. While the mining industry recognizes that particle shape profoundly affects operational performance, the transition from qualitative awareness to quantitative prediction remains an active research frontier. The absence of continuous 3D shape analysis has been the rate-limiting factor preventing this progression. This research provides the technological foundation to overcome this barrier, enabling the next generation of shape-integrated operational models. Analyzing the angularity, sphericity, and elongation of particles can enhance the efficiency of processes such as blasting, loading and hauling, crushing, and grinding, ultimately reducing operational costs from the mine to the mill.

1.2. What this research offers

This study builds directly on our previous work (Faramarzi and Esmaeili, 2025), which primarily analyzed rock fragmentation based on particle size distribution. While our earlier study offered valuable insights into 3D rock fragmentation analysis under suboptimal lighting, it highlighted a critical gap in the limited understanding of particle shape characteristics. The present study aims to address this shortcoming by demonstrating both the significance and practical feasibility of incorporating shape analysis into conventional particle size distribution studies, thereby offering a more comprehensive approach to fragmentation assessment.

We argue that while particle size is a crucial factor in mining and milling, morphological characteristics of rock particles are equally significant for optimizing material handling and improving processing efficiency. The offered method needs to be robust in all lighting situations, including bright sun in the day, shadows in the evening, or a lack of optimal light at night shifts and in underground mines. To overcome the challenges of quantitatively analyzing particle shape robust to lighting scenarios, this study applies a novel approach leveraging LiDAR technology and deep learning-based point cloud segmentation (presented in Faramarzi and Esmaeili (2025)) for accurate and comprehensive 3D shape analysis. Unlike traditional 2D image-based techniques, the proposed approach provides a robust, precise and quantitative characterization of particle shape factors, such as angularity, sphericity, aspect ratio and longest dimension. The developed method is also robust to lighting conditions, as laser scanners are typically independent of external light sources, emitting and detecting their own light. By offering a scalable and efficient solution, this research aims to enhance the characterization of fragmented rock material across various material handling systems, improve energy consumption management in mills, and contribute to safer and more cost-effective mining practices through morphological analysis of the particles. A graphical representation of the research is provided in Fig. 2.

Fig. 2 presents the complete methodological pipeline of this research, illustrating the integration of synthetic data generation, deep learning-based segmentation, and experimental validation for 3D shape analysis. Using Blender's 3D modeling environment, we create diverse rock piles with controlled geometric properties and collect labeled point cloud data of the pile. This automated labeling process circumvents the prohibitively expensive and time-consuming task of manually annotating real point cloud data, while simultaneously enabling precise control over data diversity to enhance model generalization.

The next stage is to train a deep learning model to segment

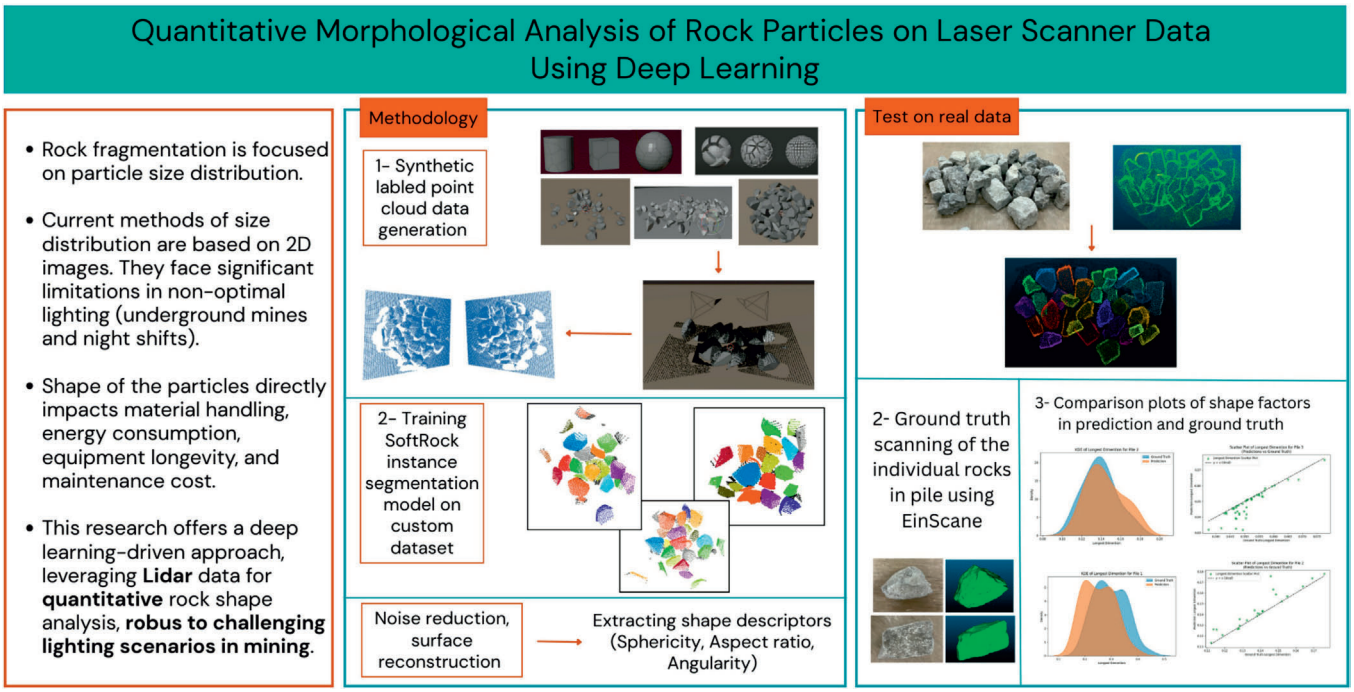

Fig. 2. Graphical representation of the research.

individual rock instances from point clouds. Following segmentation, shape descriptors including sphericity, aspect ratio, angularity, and longest dimension are computed for each identified rock fragment. The next stage validates model performance through experimental testing real rock piles scanned with a Leica laser scanner. Each rock in a pile was individually scanned using an EinScan device to establish ground truth shape measurements, enabling quantitative comparison between predicted and actual shape factor distributions through metrics including cumulative distribution plots, scatter diagrams, and statistical error measures. This systematic workflow, from synthetic data generation through real-data validation, establishes a reproducible framework for integrating quantitative 3D shape analysis into operational workflows.

2. Literature review

2.1. Computer vision methods for particle size distribution analysis

Numerous techniques have been developed for measuring particle size distribution, with digital image analysis, encompassing both classical and advanced approaches, becoming a widely adopted, efficient, and cost-effective method. Classical image processing methods, although practical and useful for analyzing rock fragmentation, often rely heavily on the visual characteristics of the training data, which can introduce bias and limit generalization (Yang et al., 2020; Guo et al., 2022). Some researchers have also employed point cloud analysis using classical methods that address some of the limitations in image processing. Other studies have utilized Unmanned Aerial Vehicles (UAVs) and photogrammetry to provide continuous monitoring and assess blasted block size distribution (Bamford et al., 2020). According to Wang et al. (2021), since current methods overlook three-dimensional shape features, such as concavity and convexity, they misrepresent true, complex shapes of the fragmented rock, leading to inaccurate assessments of fragment sizes. They incorporated laser scanner data to address this issue; however, classical models and manual feature extraction methods are tailored to specific mines and are not generalized to different mining environments and geological variations.

Modern deep learning-based approaches using RGB images and photogrammetry have demonstrated greater generalization across different mining environments and rock textures (Bamford et al., 2021; Ikeda et al., 2023; Schenk et al., 2019; Wang et al., 2021; Yang et al., 2021; Zyuzin et al., 2021). However, like classical methods, they are constrained by their reliance on RGB features, lighting and image quality. Variations in lighting, weather conditions, night shifts, and shadows in rock piles can compromise the accuracy of these models, limiting their performance in the unpredictable environments often encountered in mining operations. To address this lighting limitation, Faramarzi and Esmaeili (2025) presented a learning-based point cloud segmentation method by directly analyzing LiDAR Data for size distribution. Their results demonstrated the model's robust performance, independent of lighting conditions, highlighting its potential for analyzing size distributions in underground mining and night shift applications in open pit mines.

2.2. Computer vision methods for particle shape analysis

As previously noted, many of the mentioned studies not only lack comprehensive shape analysis but also simplify particle geometries to a 2D and often circular approximation when estimating sizes in muck piles (Schenk et al., 2019). While this approach has its benefits in some aspects, it risks oversimplifying the intricate nature of particle shapes, potentially missing the impact of diverse particle shapes on operational efficiency and performance. By focusing predominantly on 2D analysis and circular approximation of shapes, these studies may lead to insufficient evaluations of how variations in particle geometry influence critical factors such as flowability and energy consumption.

The characteristics of the rock mass, such as material composition, foliation, and joint patterns, combined with the blasting methods used, typically cause rocks at a given site to break into unique irregular shapes (Unland and Al-Khasawneh, 2009). Understanding the shape of these blasted fragments is essential, as it impacts both the fracturing mechanics and bulk properties like volume and packing density. It further impacts the strength and fracture characteristics of the fragments, as well as the efficiency of mechanical sieving processes for materials like the feed for primary crushers (Li et al., 2021).

Many studies on shape analysis in various subjects and topics share the concept that shape can be effectively characterized using three primary descriptors: form (aspect ratio), roundness (angularity), and sphericity (Govender et al., 2018; Ma et al., 2022; Ulusoy, 2023; Xia, 2017). In rock fragmentation research, digital image analysis has been widely utilized to assess both the size and shape of rock fragments. This approach typically involves applying boundary detection techniques to 2D images to extract shape descriptors such as form, roundness, and angularity. These descriptors are then compiled into histograms to represent the distribution of particle shapes. By analyzing these shape characteristics, the study provided valuable insights for monitoring and optimization of rock blasting operations.

Unland and Al-Khasawneh (2009) investigated the impact of limestone particle shape on crushing parameters using a high-resolution impact analyzer. The researchers classified particles into seven shape categories, ranging from spherical and cubic to plate-like and acicular. Findings indicate that particle shape significantly influences contact time, force, energy transfer, and size distribution of the fragments. Specifically, spherical and cubic particles exhibit the highest contact forces and energy transfer, alongside the shortest contact times. Additionally, the study found that energy utilization was lowest for spherical and cubic particles, increasing with greater elongation and flatness. The analysis also included a histogram of shape distribution, revealing minimal influence of initial shape on smaller fragment sizes.

Feng and Bernhardt-Barry (2025) proposed a deep learning pipeline for granular particle shape quantification that integrates an image tiling strategy, YOLOv8 for detection, and the Segment Anything Model (SAM) for pixel-level segmentation, leading to morphological characterization of particles. The authors introduced brightness and contrast variation for data augmentation as simulating lighting scenarios in mining; however, this approach is insufficient to replicate the true complexity of natural lighting. Specifically, it fails to simulate the geometric and photometric challenges introduced by cast shadows, where the shadow of one particle completely occludes and alters the appearance of another. Such occlusion is a major source of error in real-world fragmentation analysis.

Ali et al. (2023) proposed a particle characterization approach that leverages digital imaging techniques to analyze shape and angularity. Capturing images of rock particles from multiple angles allowed for 3D geometric analysis. The approach utilized a luminous background for image processing within MATLAB, isolating individual particles and enabling the extraction of the longest and shortest dimensions of the rocks. Using these critical dimensions, the elongation, flatness, and angularity are quantified through mathematical equations derived from the particle contours.

Shape analysis in mining has garnered attention in earlier studies, but a significant gap in research on this topic existed until more recently. Recently, Ma et al. (2022) explored the quantitative analysis of fragment morphology resulting from rock grain crushing. The researchers used a 3D scanner to capture the intact grain morphology and applied the finite-discrete element method (FDEM) to simulate the fragmentation process. Angularity and sphericity were calculated using geometric parameters derived from the 3D reconstructed fragments. Their findings highlight variations in fragment sizes and shapes between rounded and angular grains, emphasizing that higher sphericity correlates with smaller fragments, while larger fragments tend to be more angular.

Despite the recognition of particle shape as a key factor in optimizing material handling, processing efficiency, and equipment longevity, existing studies in rock fragmentation have primarily emphasized size distribution. Methods for shape analysis remain limited, especially in their ability to capture the irregular, three-dimensional geometries of blasted rock fragments across a broad size range. Current 2D image-based approaches often struggle with lighting conditions, occlusions, and depth ambiguity, making them unsuitable for detailed shape characterization in operational environments. Using a 3D scanner can mitigate this issue, as Ma et al. (2022) employed 3D scanning methods to analyze the effect of shape on fragmentation. However, the application of the finite-discrete element method (FDEM), as it is used in this research, is computationally demanding and resource-intensive, which can hinder real-time implementations.

To address these limitations, this research applies a novel framework that integrates LiDAR technology with deep learning for comprehensive 3D shape analysis of blasting fragments. In doing so, it overcomes the constraints of traditional imaging by providing lighting-invariant, spatially accurate models of particle morphology. This methodology moves beyond the constraints of 2D analysis, offering a robust characterization of particle shape alongside size, thereby promising enhanced understanding of material behavior in handling, crushing, grinding, and screening, ultimately contributing to improved operational efficiency, energy management, and equipment longevity in mining.

3. Methodology

3.1. Synthetic labeled dataset

Training deep learning models for point cloud segmentation and shape interpretation demands high-quality large, labeled datasets with diverse examples. In applications like rock fragmentation, gathering such data from real-world scenarios and annotating it is especially difficult because of the irregular and unpredictable geometry of the rocks, overlapping fragments, and common occlusion issues. These factors further complicate the time-consuming and expensive process of manual labeling, making it challenging to capture the subtle shape variations needed for detailed analysis. To overcome these obstacles, synthetic datasets generated through 3D modeling have proven invaluable.

This work uses a pioneering method in the field of mining, rock fragmentation, and shape analysis by employing synthetic data to generate labeled point clouds specifically tailored for size and shape analysis of rock piles (Faramarzi and Esmaeili, 2025). Using Blender (2022), we created 3D models with controlled size and shape features. To enhance rock diversity and boost the realism of the dataset, a range of Blender add-ons and extensions were used as well as different initial objects for fracture and adjusting parameters such as Noise and Source to control properties such as size, shape and fragmentation patterns, and occlusion in “Scene Generation” section. In “Scanner” section (Reitmann et al., 2021), we were also able to define key sensor properties, such as visual scope, point density, and sensor noise as well as number and location of the scanners. This approach allowed us to generate a labelled point cloud that not only represents realistic rock shapes but also accounts for the inherent imperfections and data variations of actual laser scanning devices. The ability to simulate realistic environmental conditions, such as occlusion from neighboring particles (where you can create more dense piles or sparse piles), further enhances the robustness of the trained model (Fig. 3). The trainability and realism of the synthetic dataset were previously evaluated in our prior work (Faramarzi and Esmaeili, 2025), where it was used for size distribution analysis on different real rock piles. It is important to note that texture and surface roughness were not accurately replicable in the 3D Blender simulation. While we attempted to simulate rough textures by increasing noise in the scanning process, the synthetic data could only mimic particles with uncomplicated surface roughness. It is also important to note that since laser scanners struggle with capturing data from highly reflective materials like opal and polished steel, the synthetic dataset does not include these types of surfaces. Consequently, the model was trained and tested exclusively on non-reflective and non-opal materials. Fig. 3 presents examples of possible size, shape and fragmentation patterns of rockpiles generated in Blender. Also, Fig. 4 illustrates an example of a point cloud collected from the pile using the scanner.

Automated labeling is achieved by first assigning category and part identification codes to scene objects. As the virtual scanner captures points, a hit indexing function records which object each point intersects, thereby associating point data with corresponding object labels.

A dataset of more than 600 uniquely labeled synthetic rock piles was generated for training purposes. Each pile was configured to contain between 8 and 50 rocks, with individual rock sizes varying from 15 to 50 cm. To achieve a more comprehensive data coverage, we placed two scanners 2.5 m distance above the scene, in two opposite sides of the pile with a horizontal distance of 2 m between them. Fig. 5 shows two sample point clouds collected by two scanners from opposite sides of a pile. The scanner originally collects point clouds in the world coordinate frame of the scene; so, both point clouds align, and they do not require point cloud registration.

The diversity of the synthetic dataset was deliberately designed to enable model generalization across varied rock morphologies. By systematically varying fragmentation parameters, scanner configurations, and pile arrangements, we created training data spanning a wide range of particle shapes, sizes, and occlusion scenarios. However, we acknowledge inherent limitations in synthetically replicating certain natural rock characteristics. Specifically, complex micro-scale surface roughness and extreme weathering patterns cannot be fully captured through simulation. Additionally, highly reflective materials (e.g., opal, polished surfaces) were excluded from the synthetic dataset due to laser scanner incompatibility. These constraints were mitigated by: (1) training on geometric features rather than appearance-based features, providing inherent robustness to surface texture variations, and (2) validating the model on three geologically distinct real rock types, representing different formation processes and morphological

Fig. 3. Sample rockpiles with different shapes, sizes and fragmentation patterns created in Blender.

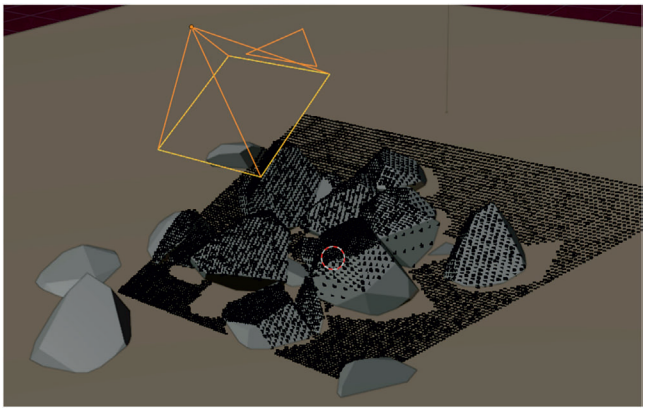

Fig. 4. Simulated pile in Blender is scanned by the scanner add-on.

characteristics. The consistent performance across these diverse materials (*MAPE*: 2%–17% for shape factors) demonstrates effective knowledge transfer from synthetic to natural rock geometries despite the acknowledged simplifications in the training data.

Using a computer with an NVIDIA RTX 3070 GPU (8 GB VRAM), a 12th Gen Intel Core i7–12700F CPU, and 32 GB of RAM, the synthetic data generation process can produce around 100 labeled piles of rock within 1–2 h, depending on factors such as rock pile scale and scanning resolution. Following dataset preparation, the data is used to train a deep learning model to segment individual rock instances in point clouds.

3.2. Transfer learning

Point clouds have become a fundamental representation for 3D data, largely due to the growing availability of acquisition devices. Since our study focuses on shape analysis, which necessitates distinguishing individual rocks, we employed instance segmentation to enable detailed examination of each rock's shape and size. Originally developed for 3D point cloud instance segmentation and trained on the ScanNet (Dai et al., 2017) dataset, SoftGroup (Vu et al., 2022) is designed to handle complex and noisy environments. The SoftGroup architecture employs a two-stage approach that combines bottom-up grouping with top-down refinement to achieve robust instance segmentation in complex, noisy environments. At its foundation, the network utilizes a U-Net-style sparse convolutional backbone that processes voxelized point clouds to extract hierarchical geometric features at multiple resolutions.

The feature extraction stage consists of two parallel branches that process the hierarchical features simultaneously. The semantic branch predicts per-point class probabilities using cross-entropy loss, while the offset branch predicts 3D offset vectors that point from each point toward its corresponding instance center, optimized through L1 regression loss. The bottom-up grouping stage clusters points into preliminary instance proposals based on three criteria: semantic predictions, offset vector similarity, and spatial proximity. A critical distinction of SoftGroup is its use of soft assignments rather than hard clustering. Each point receives probabilistic association scores with multiple candidate instances rather than binary membership, providing inherent robustness to noise and ambiguous boundaries. This characteristic is particularly valuable for analyzing rock piles where particle boundaries may be unclear due to contact points, occlusion, or sensor noise.

The top-down refinement stage employs a second U-Net network to validate and refine the preliminary proposals generated by the bottom-up grouping. This stage pools features from points within each proposal region to create per-instance feature representations. Three specialized prediction heads then process these features: a classification head validates instance proposals to distinguish true classes from spurious noise clusters, a mask scoring head predicts confidence scores for each instance mask, and a bounding box regression head refines 3D bounding boxes around instances. The refinement stage is trained using three complementary loss functions: binary cross-entropy mask loss, L1 center loss, and IoU bounding box loss. This multi-task learning approach ensures that the model learns to accurately delineate instance boundaries while maintaining precise localization.

To tailor the model to our specific dataset, we applied transfer learning by fine tuning and adjusting configuration parameters. Model hyperparameters such as voxel size and clustering features (radius and min-max number of points) originally optimized for indoor scene segmentation required adjustment for rock pile analysis. The semantic classification was simplified to two classes (rock and floor) with a single instance class (rock), reflecting the focused application compared to the 20 + categories in ScanNet indoor scenes.

The dataset structure mirrors the format of ScanNetv2 to ensure compatibility. We divided our labeled dataset into training (75%), validation (15%), and testing (10%) subsets. A batch size of 4 was selected, following recommendations from the original model and considering GPU memory constraints. The model was trained using the Adam optimizer with a learning rate of 0.004, which was determined based on the original configuration and tested through a basic random search. We initialized training using the pretrained HAIS weights available on the SoftGroup GitHub repository. This transfer learning and fine tuning resulted in a customized version we refer to as SoftRock (Faramarzi and Esmaeili, 2025).

The proposed method was trained and tested using the computer mentioned in Section 3.1. Model training on the synthetic data required around 10 h, whereas inference time varied from 1 s for smaller and sparser point clouds to approximately 30 s for larger, more complex ones, demonstrating its potential for real-time applications. Fig. 6

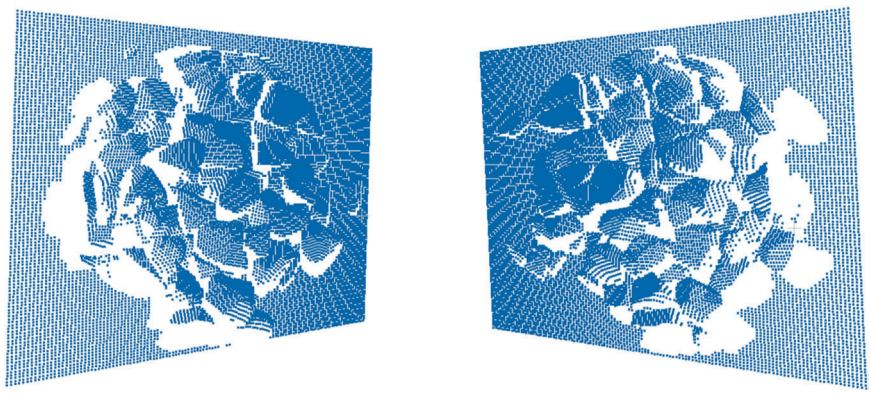

Fig. 5. Point clouds captured from the same rock pile using two scanners at opposite sides.

Fig. 6. Segmentation results for the three test point clouds of the rock piles are visualized.

presents the model's performance in segmenting individual instances for three test samples of rock piles. Each detected rock is visualized in a different color.

3.3. Instance segmentation evaluation of SoftRock model

To measure the accuracy and reliability of instance segmentation algorithms, several evaluation metrics are regularly utilized. For semantic segmentation tasks, Accuracy (*Acc*: the proportion of correctly classified points) and mean Intersection over Union (*mIoU*: provides an overview of segmentation performance across different categories) are widely applied. In the instance segmentation task, more specific metrics such as Average Precision (*AP*: a comprehensive measure of how well the model detects distinct instances) and Average Recall (*AR*: providing insight into the model's effectiveness in recalling instances at various *IoU* thresholds) are utilized. *RC*_50% and *AP*_50% specify the recall/precision at 50% *IoU* thresholds.

Evaluating segmentation metrics for rock fragmentation analysis currently lacks a standardized benchmark, especially for methods based on point clouds. While a few image-based analysis approaches have recently reported *IoU* Zhao et al. (2024) *IoU* of 94.4% and Wang et al. (2021) *IoU* for the ore mask 86.95%, *IoU* for the ore boundary 52.32%, their structured data and performance characteristics differ significantly from those of point clouds. Unlike image segmentation, which leverages dense, uniform grid data and a mature research field to achieve *IoU* scores often above 90%, point cloud segmentation contends with sparse and irregular data. Due to these fundamental differences and a relative scarcity of pre-trained models and benchmarks, its typical *IoU* performance of 70–80% is considered a robust outcome.

Using the specified evaluation metrics above, we assessed the model's segmentation performance by comparing the predicted labels with the ground truth labels on a 10% unseen test dataset. On this test dataset, the model achieved a mean Intersection over Union (*mIoU*) of 76.5% for semantic segmentation. For instance segmentation, it reached an Average Precision (*AP*) of 62.8% and a Recall (*RC*) of 68.2% at a 50% *IoU* threshold. These results underscore the potential of point cloud segmentation as an effective way to overcome the lighting-related issues of image-based techniques. The study, in conjunction with the proposed dataset generation platform, thus represents a significant advancement in establishing standardized benchmarking practices for point cloud-based rock fragmentation analysis.

With individual rocks now identified, the subsequent step involves shape analysis and comparing these results against ground truth data. The following section will detail this shape analysis, involving the computation of shape factors for both predicted and real labels.

3.4. Shape analysis and evaluation metrics

Having a 3D point cloud of each instance enables us to observe the shape of the detected rocks accurately. As mentioned, different shape factors can be measured, among which we studied the shape analysis of the data using the following metrics.

Sphericity: Sphericity (circularity in 2D) evaluates the 3D compactness of an object and its similarity to a perfect sphere. It is calculated as:

$$S = \frac{\pi^{\frac{1}{3}} (6.\ Volume)^{\frac{2}{3}}}{Surface\ Area} \tag{1}$$

Where the volume quantifies the object's spatial properties and surface area describes its boundary features. A sphericity value of 1 indicates a perfect sphere, while deviations from this value suggest increasing irregularity and jagged shape.

Angularity: Angularity refers to the sharpness or pointiness of a particle's edges and corners. It quantifies how rough or jagged the edges are. Angular particles have sharp corners and well-defined edges, and tend to have a higher angularity index due to the presence of more pronounced, sharp features. Conversely, particles with low angularity are smoother, with more rounded corners and less defined edges, often resulting from weathering or extended transport. One method to quantify angularity is the Surface Area-Based Angularity Index, which calculates the difference in surface area between the actual particle and a hypothetical sphere that has the same volume. The index is defined as:

$$\text{Angular Index} = \frac{A_{Actual} - A_{Sphere}}{A_{Sphere}} \tag{2}$$

where A_{Actual} refers to particle's true surface area, and A_{Sphere} represents the surface area of an equivalent-volume sphere.

Feret Diameter: Feret diameter of an object, also known as the maximum Feret length, is the longest possible distance between any pair of parallel tangents drawn to its outline. It provides a key measure of an object's characteristic length and mathematically represents the maximum pairwise Euclidean distance between boundary points. Since for a convex shape, the Feret diameter is very close to the longest dimension, we use the longest dimension and the Feret diameter in this text interchangeably.

Aspect Ratio: The aspect ratio can be defined in two ways: (1) as the ratio of length to width, providing a general sense of how elongated a particle is, and (2) as part of dimensional ratios that capture flatness. Since elongation is more likely to cause blockage than flatness, we focus on elongation in this study. Higher aspect ratios indicate more elongated shapes, while lower values suggest more compact forms (Fig. 7).

With the aforementioned shape descriptors and the point cloud

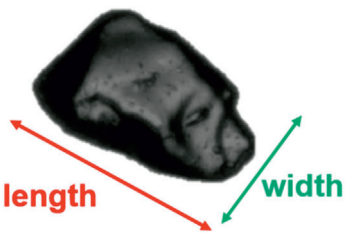

Fig. 7. Length and width of the particle.

segmentation results from the previous step, we can analyze the shape of the segmented particles. The following evaluation metrics are used on the shape results to provide a comprehensive assessment of the shape factor distributions:

KDE (Kernel Density Estimation) Diagram: A non-parametric method for estimating and visualizing the probability density function of a dataset, often used to compare the distribution of predicted shape factors against the ground truth. High accuracy is indicated when the two curves share similar peaks, spreads, and overall shape. Quantitative measures, such as the Wasserstein Distance, can be used alongside KDE to numerically assess the closeness between distributions.

Wasserstein Distance (WD): A statistical measure that quantifies the difference between two probability distributions, offering insight into how closely the predicted shape factor distribution aligns with the ground truth. A lower WD value indicates a closer match, with values below 0.1 typically suggesting a strong alignment in normalized shape distributions; however, acceptable thresholds can vary depending on the application and data scale.

Scatter Plot: A graphical representation that displays the relationship between predicted and ground truth values, helping to visualize trends, correlations, and potential deviations in the model's predictions.

MAPE (Mean Absolute Percentage Error): A widely used regression metric that quantifies the average absolute difference percentage between predicted and actual data. It provides an intuitive measure of prediction accuracy, where lower values indicate less percentage error and a better model performance. A *MAPE* below 10% is generally considered highly accurate.

Fig. 8 presents the shape analysis results of Angularity and Sphericity for the segmented test synthetic rock pile sample. For Angularity, the model demonstrated a moderate level of accuracy, with a Wasserstein Distance of 0.2102 and an *MAPE* of 12.37%. The scatter plot indicates a reasonable clustering of data points around the ideal y = x line, suggesting a fair agreement between predicted and ground truth values. The model performed with higher precision in predicting Sphericity, achieving a Wasserstein Distance of 0.0425 and an *MAPE* of 6.01%. The scatter plot reveals a strong alignment of data points along the y = x line, and the KDE plot confirms a close overlap between the predicted and ground truth sphericity distributions. The mean predicted Sphericity (0.6937) is slightly lower than the mean ground truth (0.7360), suggesting a minor underestimation.

The precision of these estimations is also impacted by factors inherent to point cloud data generation. The noisy nature of the point cloud, introduced during data acquisition, can create small surface deviations that distort local geometric features, directly affecting the precision of both angularity and sphericity estimations. Additionally, while the convex hull method is used to define the overall shape for sphericity, it can struggle to precisely capture intricate surface details and indentations, leading to a minor oversimplification of the particle's true shape. Finally, occlusions, where one particle is hidden by another in the pile, present another challenge by providing incomplete point clouds for certain particles, further contributing to potential inaccuracies in shape analysis. These factors collectively contribute to the observed differences between the predicted and ground truth values.

Fig. 9 presents the analysis of the Test Pile's Longest Dimension and Aspect Ratio. For the longest dimension, the model demonstrated high accuracy, with a Wasserstein Distance of 0.0599 and an *MAPE* of 3.98%. The scatter plot shows a reasonable clustering of data points around the ideal y = x line, indicating a strong agreement between predicted and ground truth values. However, the KDE plot suggests a slight shift towards lower predicted longest dimensions, and the mean predicted Longest Dimension (0.6103) is slightly lower than the mean ground truth (0.6240). In contrast, the Aspect Ratio exhibited higher prediction errors, with a higher Wasserstein Distance of 0.7145 and an *MAPE* of 16.92%. This discrepancy is a result of fundamental challenges in rockpile characteristic estimation, specifically occlusion and incomplete sensor views. When one particle is hidden behind another, or when the scanner's field of view fails to capture all sides of a rock, the resulting point cloud is incomplete. This can significantly impact the calculation of all three dimensions (longest, intermediate, and shortest), which are necessary for determining the aspect ratio. This effect is particularly pronounced in the aspect ratio where one dimension is divided by another, thus propagating any errors from the initial measurement. For instance, the scatter plot shows a single rock with a very high aspect ratio value. This is likely a result of an incomplete scan, where only one surface of the rock was captured, causing its shortest dimension to be severely underestimated. This issue likely also accounts for the deviation observed in other shape factors (Sphericity and Angularity) measurements for that specific rock.

4. Model performance on experimental data

4.1. Experimental setup and scanning

Following initial training and evaluation on synthetic datasets, the model was tested on real-world LiDAR data to thoroughly validate its shape analysis capabilities. To thoroughly evaluate the model's scalability, we curated three distinct rock piles in a laboratory setting, each presenting unique particle sizes, shapes, and geological characteristics. A Leica Scanner was used to scan these rock piles (Fig. 10).

Blasted rocks from a limestone quarry, with particle dimensions spanning 15 cm to 30 cm were used as the first rock pile. The second pile collection consisted of rounded pebbles, ranging in size from 8 cm to 15 cm. Finally, the third pile consisted of crushed copper ore particles of Andesitic composition, sampled directly from a conveyor belt, with sizes varying from 3 cm to 7 cm. These three diverse piles were deliberately chosen to represent a broad spectrum of rock types, each displaying unique textures and colors. Their varying size distributions and particle geometries further underscore the different sources and environments they represent, enabling a robust assessment of the model's adaptability and performance under varied conditions.

The piles were scanned using a Leica Nova MS50 Total Station from a distance of 1.2–1.5 m, with the scanner positioned at a height of approximately 160–170 cm. Each pile was scanned from four various perspectives (e.g., from the north, south, west, and east aspects of the pile). To assess the scalability of point cloud density, scans were conducted under varying settings. The densities of the resulting point clouds were 49,202 for Pile 1, 92,332 for Pile 2, and 34,574 for Pile 3.

4.2. Establishing ground truth data

Ground truth for assessing model accuracy was established by acquiring high-resolution 3D meshes of individual rock samples with an EinScan device (Fig. 11). Each rock was physically removed from the pile and scanned in isolation, ensuring complete 3D surface coverage free of occlusion and providing instance-level shape measurements as the reference for model evaluation.

For each extracted mesh, key shape metrics (angularity, sphericity, the longest dimension, and aspect ratio) were calculated. These shape factors serve as a reference for evaluating the model's performance and validating its ability in shape analysis.

4.3. Model segmentation results and qualitative assessment

4.3.1. Point cloud segmentation

To analyze the rock fragmentation, the point clouds collected in Section 4.1 were input into the SoftRock model for individual rock segmentation and subsequent shape factor computation. The segmentation results for Piles 1, 2, and 3 are displayed in Fig. 12.

4.3.2. Shape analysis results for pile 1

Fig. 13 shows the Angularity and Sphericity of Pile 1. In the angularity analysis of pile 1, the model demonstrated strong accuracy, with a

Test Pile

Angularity

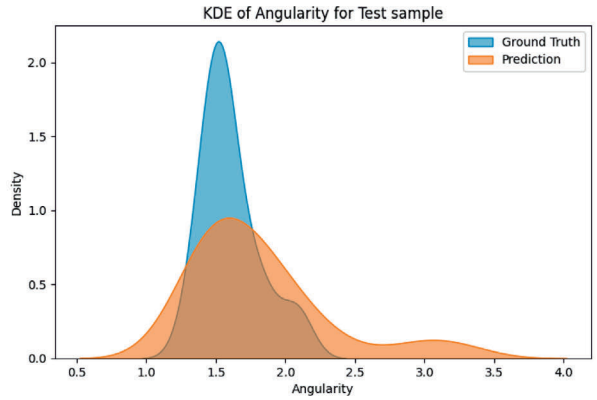

Wasserstein Distance: 0.2102

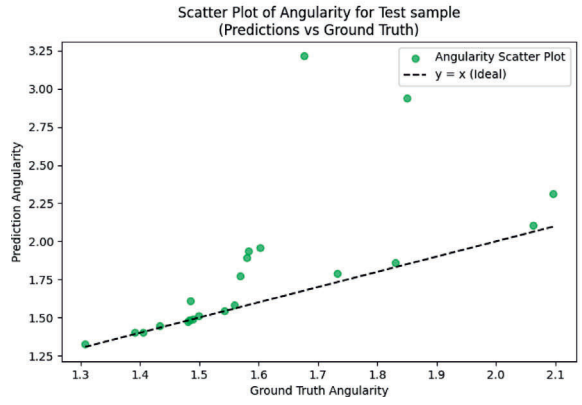

MAPE = 12.37%

	Ground Truth	Prediction
Mean	1. 6030	1. 8126
Std	0. 2026	0. 4829

Sphericity

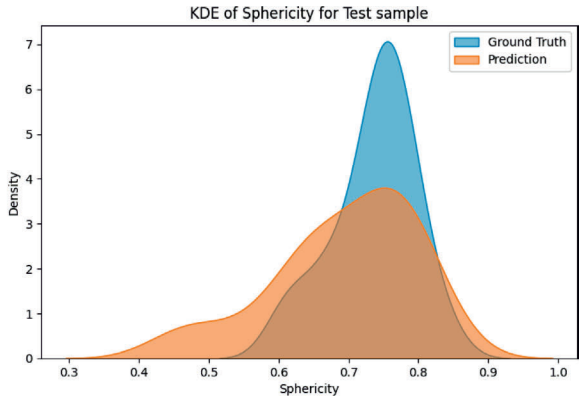

Wasserstein Distance: 0.0425

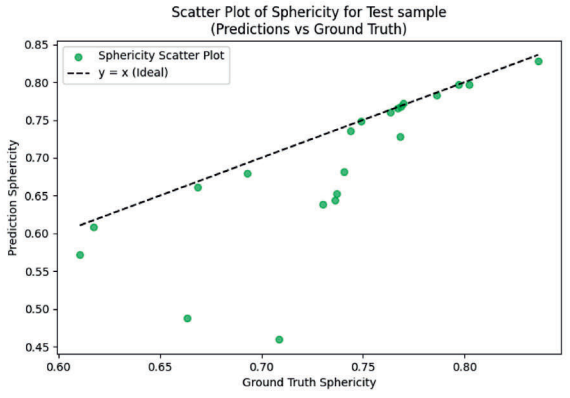

MAPE = 6.01%

	Ground Truth	Prediction
Mean	0. 7360	0. 6937
Std	0. 0570	0. 0983

Fig. 8. Test pile: analysis of angularity and sphericity.

Test Pile

Longest Dimension

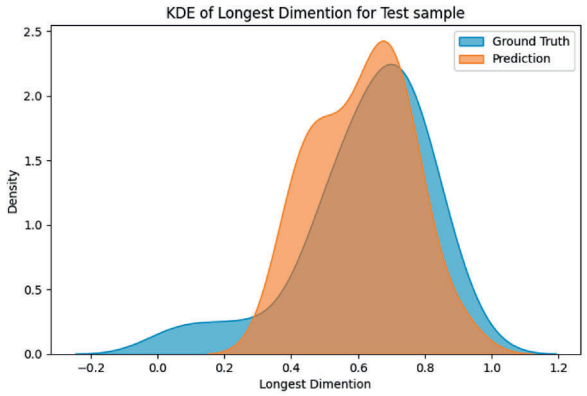

Wasserstein Distance: 0.0599

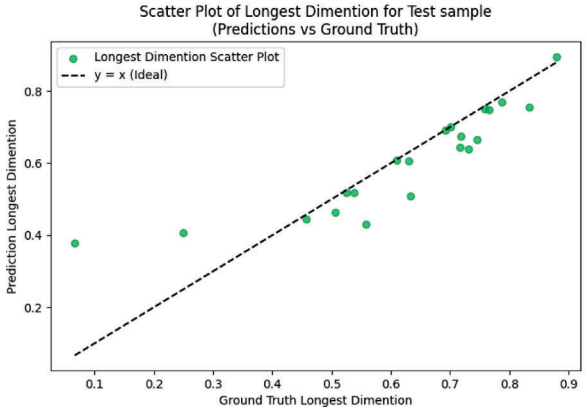

MAPE = 3.98%

	Ground Truth	Prediction
Mean	0. 6240	0. 6103
Std	0. 1880	0. 1369

Aspect Ratio

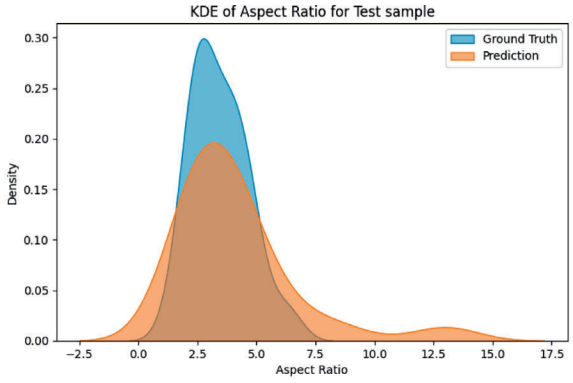

Wasserstein Distance: 0.7145

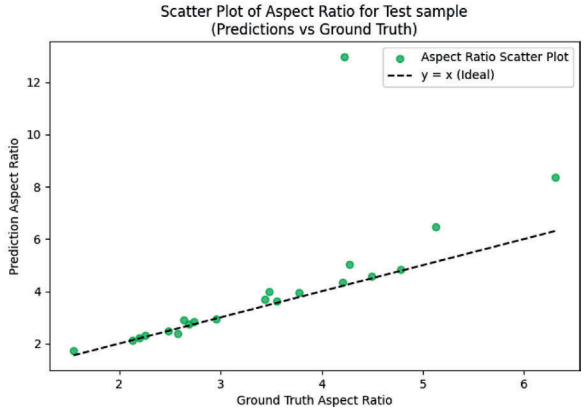

MAPE = 16.92%

	Ground Truth	Prediction
Mean	3.4238	4.1170
Std	1.1506	2.5162

Fig. 9. Test pile: analysis of longest dimension and aspect ratio.

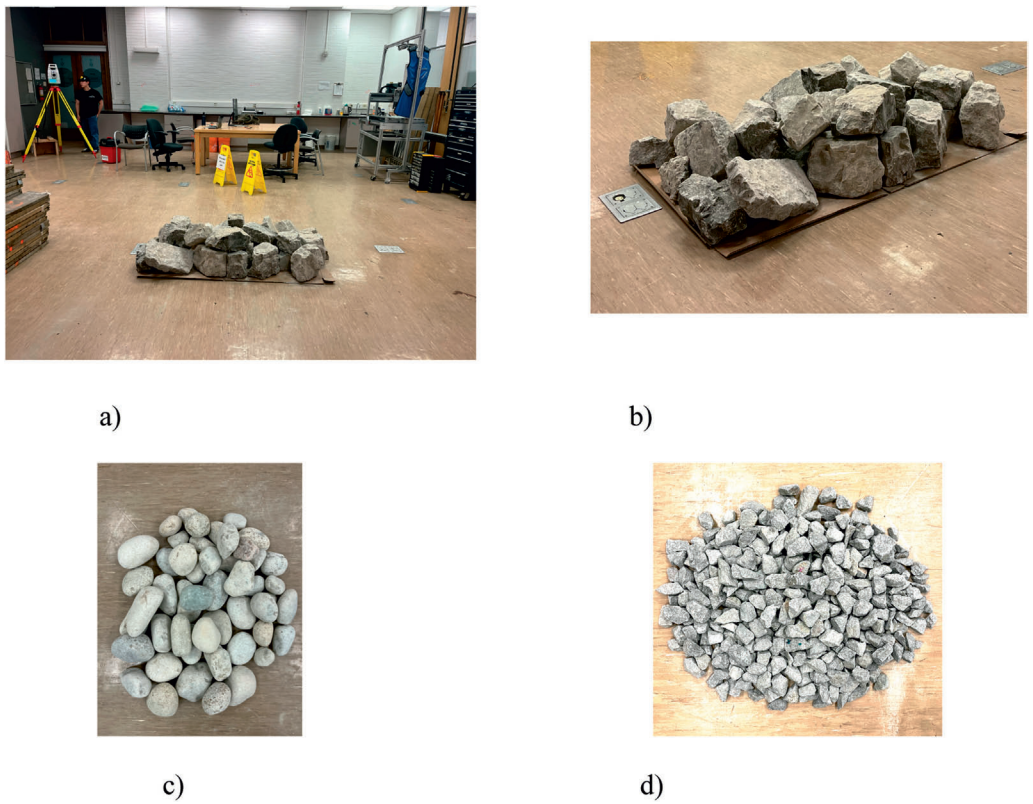

Fig. 10. Experimental setup and rock piles. (a) Leica Scanner positioned for data collection in the lab. (b) Pile 1: blasted rocks. (c) Pile 2: rounded pebbles. (d) Pile 3: crushed copper ore particles.

Wasserstein Distance of 0.1406 and an *MAPE* of 9.00%. The scatter plot shows a clustering of data points along the ideal y = x line, indicating a good agreement between predicted and ground truth values. This is further supported by the KDE plot, where the distributions of predicted and ground truth angularity largely overlap, albeit with a slight shift toward lower predicted values, due to noise. For sphericity, the model performed with high precision, achieving a Wasserstein Distance of 0.0524 and an *MAPE* of 6.96%. The scatter plot reveals a strong alignment along the y = x line, while the KDE plot confirms a good overlap between predicted and actual distributions, suggesting the model effectively captures the uniformity of the rock shapes.

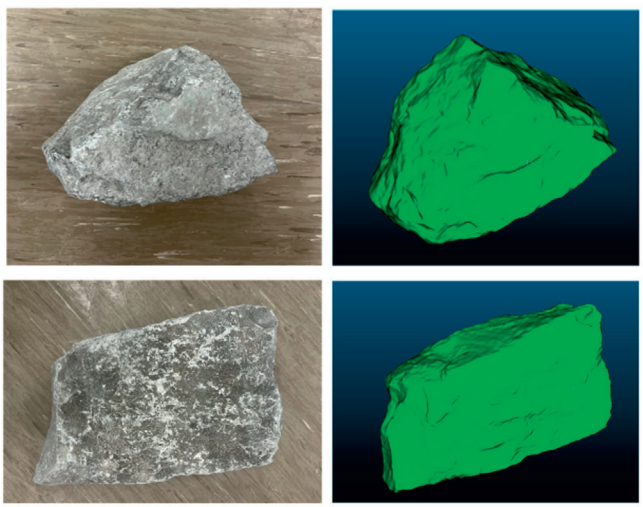

Fig. 11. Two rock samples (left) with their digital representations acquired via EinScan (right).

As discussed earlier, the errors in shape metrics arise from the noisy nature of the point cloud, the occlusion issues and particle overlap within the rock pile, restrictions in sensor view, and the inability of the convex hull to fully capture the intricate details of the particles' surface geometry. Aspect Ratio and Longest Dimension rely on distance-based measurements that are inherently robust to local surface noise. In contrast, Sphericity and Angularity are calculated from surface area measurements, which are highly susceptible to local geometric perturbations introduced by sensor noise. Sphericity compares surface area to volume, requiring accurate reconstruction of the entire particle envelope, making it moderately sensitive to missing data from occlusion or scanning shadows. Angularity is the most noise-sensitive metric, as it measures local surface curvature deviations through second-order derivatives; This fundamental difference explains why distance-based metrics outperform surface-integral metrics in shape characterization. As illustrated in Fig. 14, noise manifests as spurious points in close proximity to the true surface, artificially increasing the apparent surface roughness and thereby inflating angularity indices while reducing sphericity values. The blue line defines the actual rock points, while the red line defines the added noise that could be considered as a rock mistakenly. As shown, the presence of noise on the surface introduces extra and irregular points, resulting in misleading angularity and sphericity measurements. The model handles some of it, but the results are still affected by noise. While using a more accurate scanner could moderate this issue, it cannot eliminate it entirely, as the nature of scanner data is inherently noisy. In contrast, longest dimension measurements rely on maximum pairwise distances between boundary points, which are inherently more robust to localized noise as they depend on global geometric extrema rather than surface integrals.

Several denoising methods were evaluated on the segmented instance point clouds, including Gaussian smoothing ($\sigma = 2.0$), Statistical Outlier Removal ($k = 16$ neighbors, $std_{ratio} = 2.0$), and Laplacian smoothing ($iterations = 25$, $\lambda = 1.0$, $\mu = -0.9$). Laplacian smoothing was ultimately

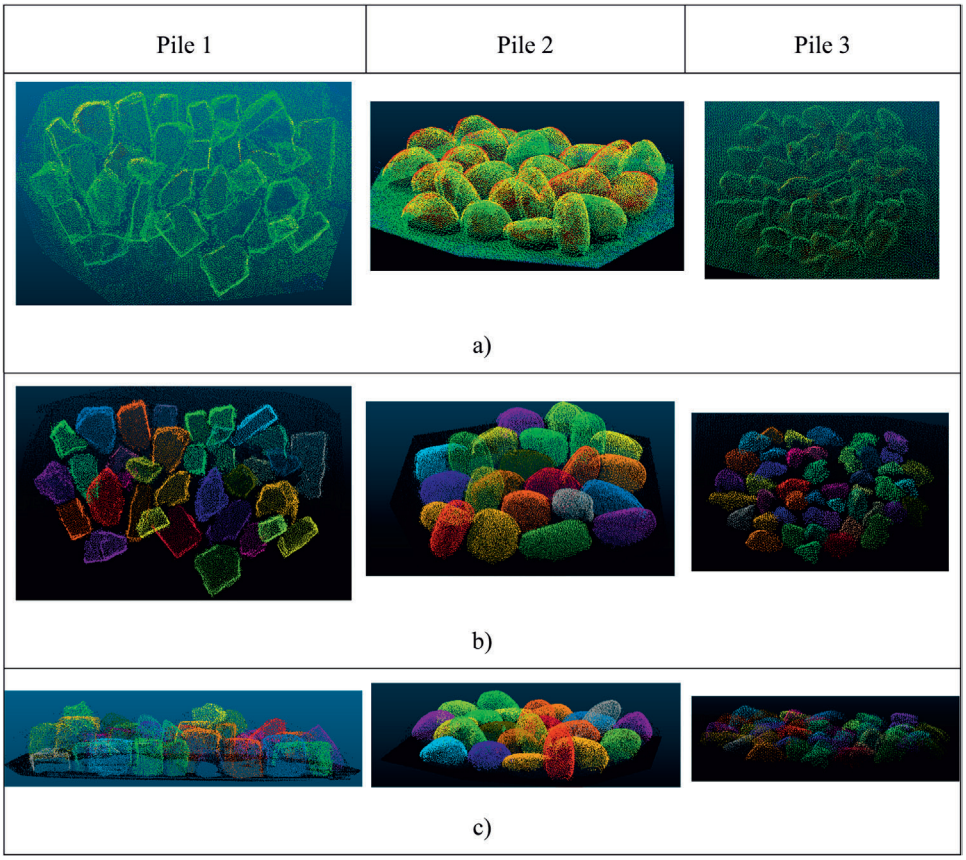

Fig. 12. Input point clouds and SoftRock's segmentation performance. (a) Raw point clouds for Pile 1 (49,202 points), Pile 2 (92,332 points), and Pile 3 (34,574 points). (b, c) Segmented rocks for each pile, derived from the SoftRock model and displayed from two different perspectives.

selected because it achieved the best balance between reducing sphericity and angularity errors and preserving geometric fidelity in measurements of the longest dimension and aspect ratio. All denoising was applied post-segmentation to individual instance point clouds.

Fig. 15 presents the effect of occlusion, which is intrinsic to analyzing rock piles. The scanner was unable to capture the complete geometry of particles occluded by others, thus introducing additional error into the measurements. Furthermore, using advanced surface reconstruction methods can help moderate the errors stemming from the convex hull's shape estimation and also improve the removal of noise.

In Fig. 16, the Longest Dimension analysis showed a reasonable level of accuracy, with a Wasserstein Distance of 0.0422 and an *MAPE* of 13.40%. The scatter plot indicates a moderate clustering of data points around the y = x line, and the predicted mean (0.2525) closely approximates the ground truth mean (0.2947). This suggests the model reliably estimates the maximum linear extent of the rocks. Also, the Aspect Ratio exhibited low prediction errors, with Wasserstein Distance of 0.0605 and a small *MAPE* of 4.75%.

4.3.3. Shape analysis results for pile 2

In the angularity analysis of pile 2 (Fig. 17), the model demonstrated good accuracy (Wasserstein Distance: 0.1219, *MAPE*: 10.97%), with scatter plots showing reasonable clustering along y = x with some outliers, and KDE plots indicating overlapping distributions, albeit with a slight shift toward higher predicted values, due to the presence of noise discussed earlier, which also affects the standard deviation. For sphericity, the model performed well (Wasserstein Distance: 0.0583, *MAPE*: 6.25%), showing a good alignment in a scatter plot (with the presence of some outliers) and the KDE plot (with a slight shift to smaller sphericity values due to loss of geometric information in data collection).

The Longest Dimension (shown in Fig. 18) was predicted with high precision (Wasserstein Distance: 0.0052, *MAPE*: 3.80%), with tight clustering along y = x and a mean prediction (0.1440) close to ground truth (0.1391). Aspect Ratio calculations also showed very low errors of Wasserstein Distance equal to 0.0376 with a high precision coverage of KDE plots, and *MAPE* of 2.71% with tight clustering along y = x in scatter plot diagram.

4.3.4. Shape analysis results for pile 3

In pile 3, for angularity (Fig. 19), the model performed well, with a Wasserstein Distance of 0.0514 and an *MAPE* of 3.87%. However, the KDE plot indicates a slight shift in predicted values. The scatter plot indicates good alignment along y = x, with mean predictions (1.3721) slightly exceeding ground truth (1.3216) due to the noise. For sphericity, the model achieved high accuracy (Wasserstein Distance: 0.0196, *MAPE*: 2.37%). The scatter plot shows strong alignment and KDE distributions with a reasonable overlap. Mean predictions (0.8135) closely match ground truth (0.8327), with minor variations in standard deviation.

For Longest Dimension (Fig. 20), the model performed well (Wasserstein Distance: 0.0030, *MAPE*: 6.21%), with KDE plots showing strong overlap and scatter plots indicating close alignment along y = x. For Aspect Ratio, the model exhibited well performance (Wasserstein Distance: 0.0866, *MAPE*: 5.80%), with very similar and aligned KDE plots and tight scatter plot along ideal line of x = y with one outlier (caused by the occlusion effect described previously).

5. Discussion

This research underscores the fundamental role of rock particle shape analysis and its impact on various aspects of mining operations, material handling, and mineral processing. While size distribution has been the dominant metric in fragmentation studies, many studies

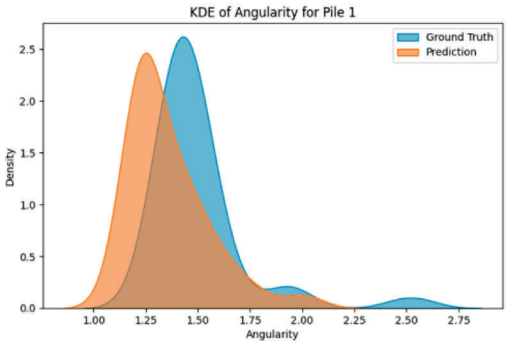

Wasserstein Distance: 0.1406

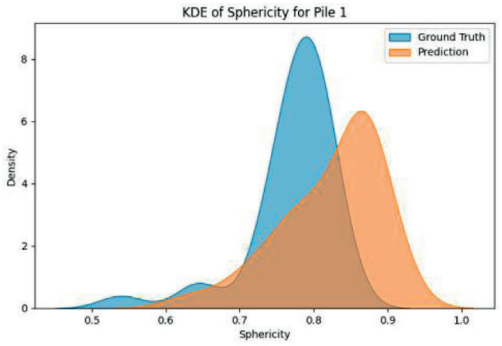

Wasserstein Distance: 0.0524

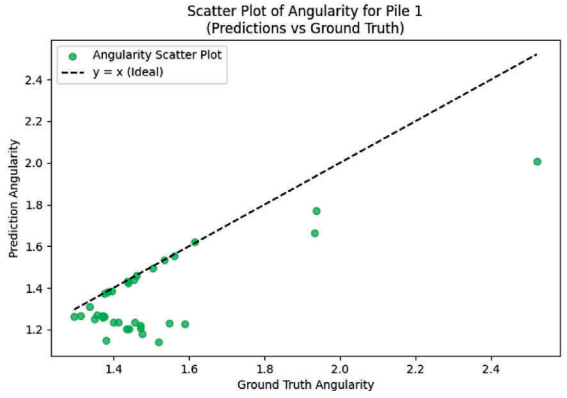

MAPE = 9.00%

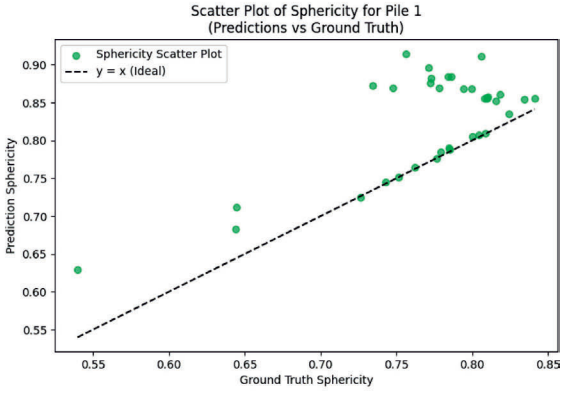

MAPE = 6.96%

	Ground Truth	Prediction
Mean	1.4979	1.3576
Std	0.2258	0.1898

	Ground Truth	Prediction
Mean	0.7710	0.8233
Std	0.0589	0.0674

Fig. 13. Pile 1: analysis of angularity and sphericity.

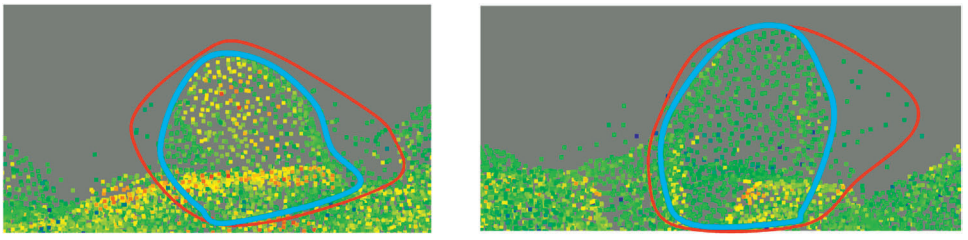

Fig. 14. The challenge of scanner noise in 3D point cloud data for two different rocks in the pile. As illustrated, some noise points exist in close proximity to the object's surface, making it difficult to accurately distinguish them from genuine surface points and potentially affecting the precise calculation of shape factors.

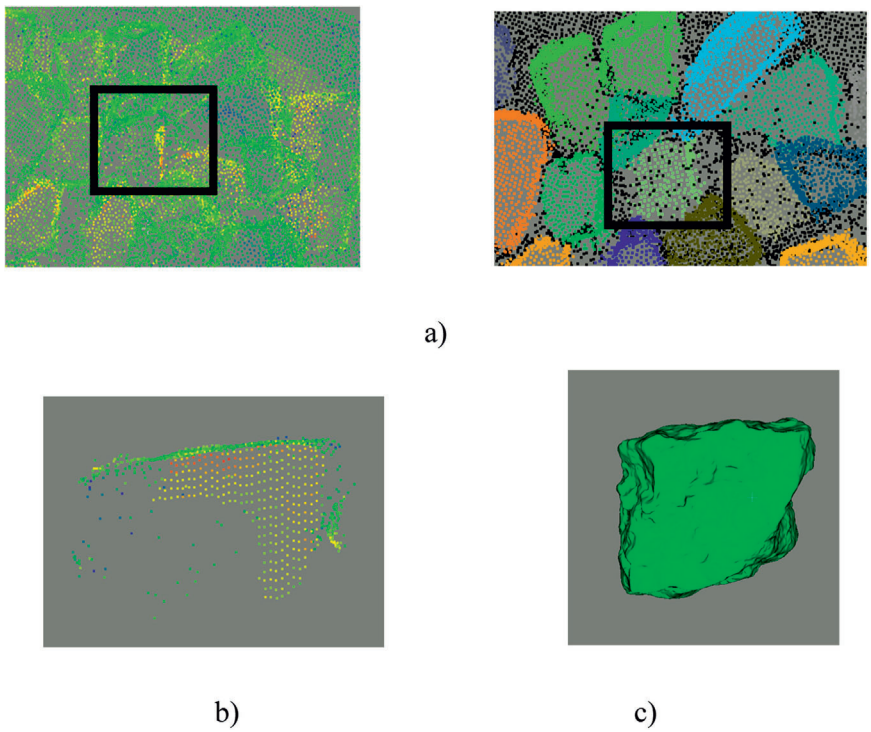

Fig. 15. Occlusion issue: a) Defined particle occluded under other top particles, b) the portion of the rock that is scanned by sensor, c) the ground truth particle.

reinforce that shape characteristics significantly influence energy consumption, equipment wear, flowability, processing efficiency and safety (Cleary and Owen, 2019; Li et al., 2021; Ouchterlony, 2003; Taylor, 2002; Wang et al., 2022; Wills and Finch, 2015). Despite the clear advantages of incorporating shape analysis, current methodologies remain constrained in their ability to accurately and efficiently characterize the three-dimensional (3D) shape of blasted rock fragments.

A key insight from this study is the direct impact of shape characteristics on mining operations. Irregularly shaped particles exhibit increased interlocking and reduced flowability, leading to material blockages in ore passes, chutes, and conveyor systems. This results in operational inefficiencies, increased maintenance costs, and potential safety hazards. Moreover, shape influences equipment wear, as angular and elongated particles contribute to higher abrasion rates in crushers, grinding mills, and transport systems. By integrating shape analysis with existing fragmentation assessments, mining operations can optimize material flow, reduce energy consumption, and enhance equipment longevity.

Previous shape analysis studies have primarily focused on specific materials, such as aggregates, rockfill, and tailings, lacking a generalized approach for the wide range of rock sizes and shapes encountered in blasting operations. Few studies on shape analysis in mining often rely on qualitative descriptions or oversimplified representations of shape. Many studies often use 2D image-based techniques, which require optimal lighting, or they employ traditional analysis methods with manual feature extraction, resulting in biased representations of particle shapes. Such shortages and oversimplifications can lead to inaccuracies in predicting flow behavior, material interlocking, and downstream processing performance.

The developed approach, which leverages LiDAR technology and deep learning-based point cloud segmentation, overcomes many of the aforementioned limitations by providing a quantitative, scalable, and light-independent method for 3D morphological characterization. To demonstrate the scalability of the model, we tested it on real rock piles from various shapes and sizes, including limestone quarries, rounded pebbles, and samples taken directly from a conveyor belt. The validation results of our shape analysis demonstrate the effectiveness of the approach in quantitatively characterizing particle morphology. By providing quantitative shape metrics alongside size distribution, we offer a more comprehensive understanding of rock fragmentation.

A critical consideration in this methodology is the generalization capacity of models trained on synthetic data. While our synthetic dataset incorporated geometric diversity through varied fragmentation patterns and scanning conditions, certain natural rock characteristics -particularly fine-scale surface roughness and weathering effects- remain simplified in the training data. The validation results across three distinct rock types with fundamentally different morphological properties provide evidence that geometric feature-based learning successfully transfers to real-world conditions. Nevertheless, future work could incorporating hybrid training approaches (combining synthetic and limited real labeled data) or domain adaptation techniques to further enhance model robustness for extreme particle geometries or unusual surface properties.

The segmentation accuracy of point cloud-based methods is inherently influenced by two interconnected factors: sensor resolution (point density) and geometric occlusion. The current model's hyperparameters, including voxel size, clustering radius, and grouping thresholds, are optimized for an average density of 20k per square meter. Extending to significantly different density regimes would require either scaling the input (and scaling back to original after segmentation) or retraining with appropriately scaled datasets. So, for applications requiring analysis of extremely high-density point clouds, strategic downsampling or architectural modifications would be necessary. Our ongoing work focuses on expanding the training dataset to encompass higher-density scenarios and exploring architectural enhancements to improve occlusion handling, ensuring scalability to large-scale field deployments.

Regarding occlusion, the SoftGroup architecture's soft assignment mechanism specifically addresses partial visibility by allowing probabilistic associations between points and instances. However, like all point cloud segmentation methods, performance degrades when particles are extensively occluded with minimal exposed surface area. Our multi-angle scanning strategy (four perspectives per pile) was designed to mitigate this limitation by ensuring that most particles have sufficient visible geometry; however, heavily occluded particles may exhibit

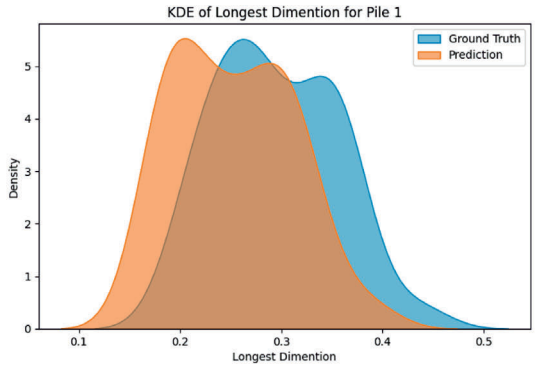

Wasserstein Distance: 0.0422

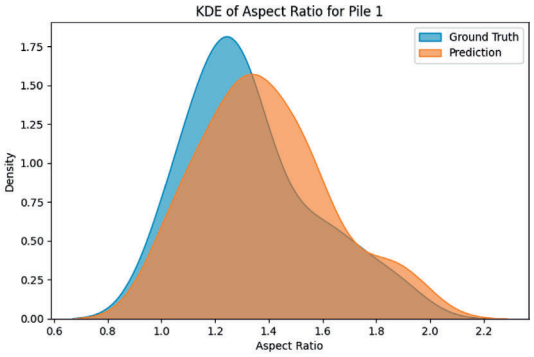

Wasserstein Distance: 0.0605

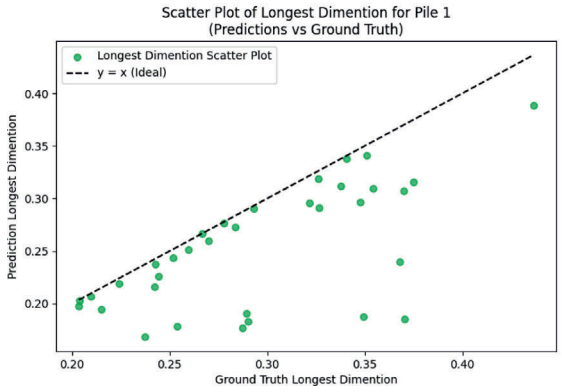

$MAPE = 13.40\%$

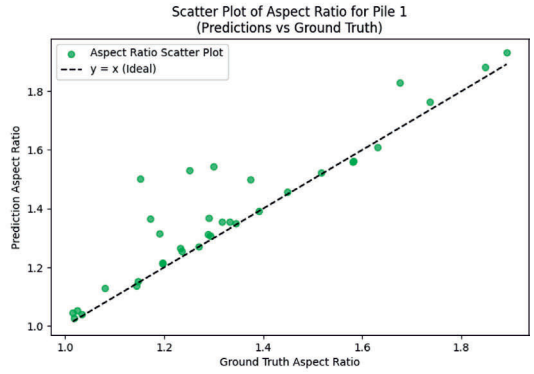

$MAPE = 4.75\%$

	Ground Truth	Prediction
Mean	0.2947	0.2525
Std	0.0583	0.0569

	Ground Truth	Prediction
Mean	1.3295	1.3857
Std	0.2296	0.2346

Fig. 16. Pile 1: analysis of the longest dimension and aspect ratio.

reduced accuracy in segmentation.

The current SoftRock implementation is optimized for particle sizes within the training distribution (15–50 cm). This approach is proven to be effective for homogeneous piles where all particles fall within a similar size range. However, this method has not been tested on highly heterogeneous mixtures containing simultaneous fine (< 5 cm) and coarse (> 50 cm) fragments within the same pile. Future work will focus on generating mixed-scale synthetic training data containing simultaneous fine and coarse particles, or alternatively, training separate models for distinct size fractions.

Discussing the results, the model demonstrated a reasonable ability to capture the key shape characteristics of the three rock piles: blasted rocks, river pebbles, and crushed ore. Some inaccuracies, such as slight underestimations or overestimations, can be attributed to noise in the point cloud data. The presence of noise in the laser scanner points cloud (on the rock surfaces) introduced errors in the analysis of angularity and sphericity. To quantify this sensitivity, we analyzed the standard deviation of prediction errors across the three test piles. Sphericity exhibited relatively lower errors (*std*: 0.0381–0.0674), while angularity showed greater variability (*std*: 0.0541–0.4829), confirming its higher susceptibility to noise-induced surface irregularities. The trade-off between noise reduction and geometric preservation is particularly

Pile 2

Angularity	Sphericity
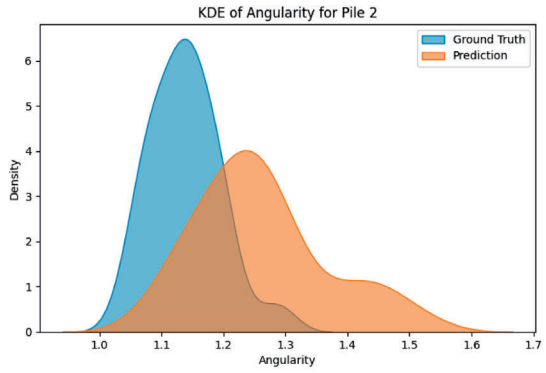	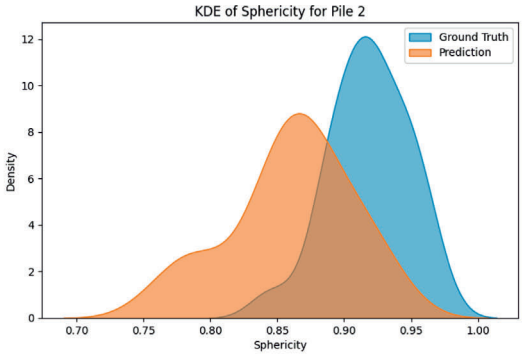
Wasserstein Distance: 0.1219	Wasserstein Distance: 0.0583
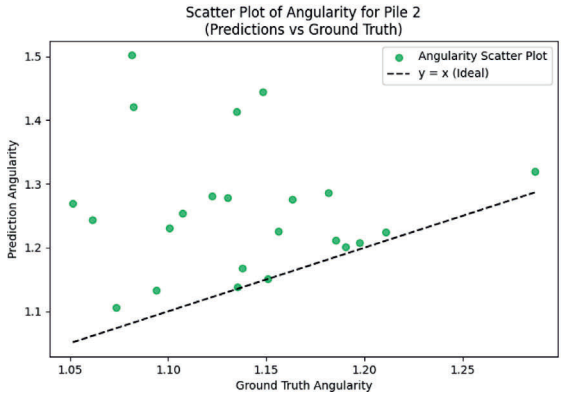	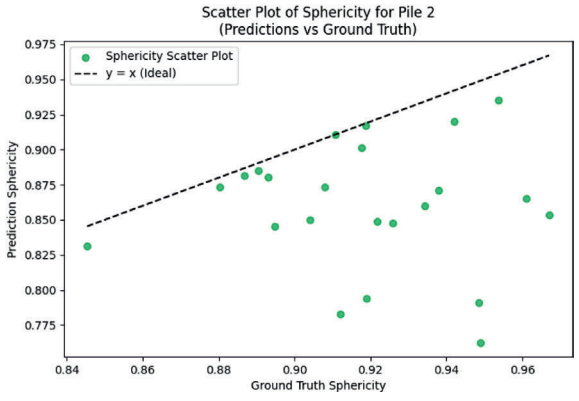
MAPE = 10.97%	*MAPE* = 6.25%

	Ground Truth	Prediction
Mean	1.1384	1.2603
Std	0.0541	0.1009

	Ground Truth	Prediction
Mean	0.9183	0.8600
Std	0. 0285	0.0441

Fig. 17. Pile 2: analysis of angularity and sphericity.

critical for angularity measurements, where authentic sharp edges must be distinguished from noise-induced artifacts.

Also, we utilized the convex hull for surface representation; however, this method proved highly sensitive to noise. Due to the arbitrary and unpredictable geometry of rock particles, conventional noise removal methods yielded suboptimal performance, occasionally leading to smoother surfaces at the cost of dimensional information loss and increased errors in aspect ratio and longest dimension. Point cloud

Pile 2

Longest Dimension

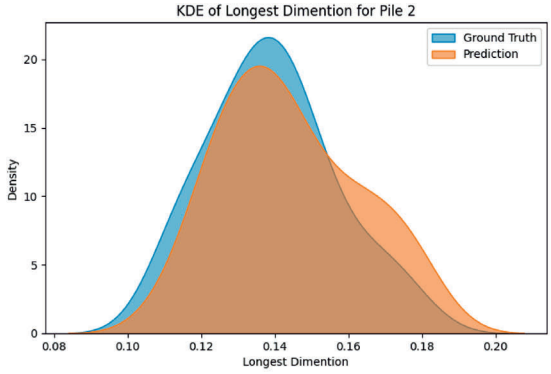

Wasserstein Distance: 0.0052

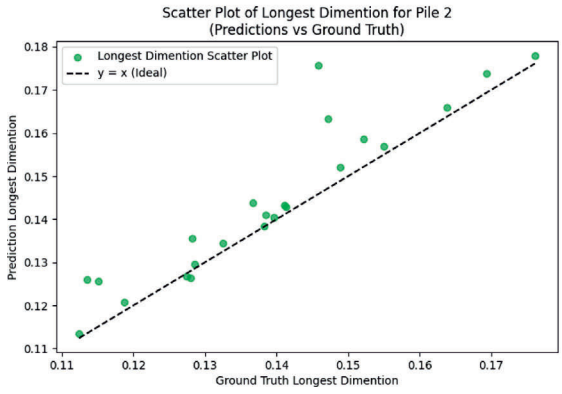

MAPE = 3.80%

	Ground Truth	Prediction
Mean	0.1391	0.1440
Std	0.0167	0.0181

Aspect Ratio

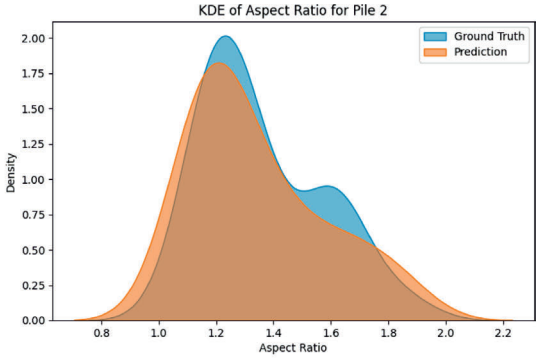

Wasserstein Distance: 0.0376

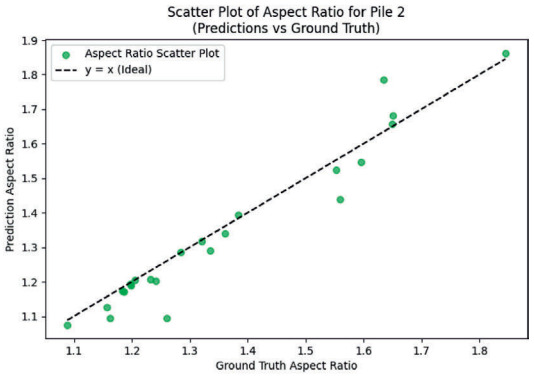

MAPE = 2.71%

	Ground Truth	Prediction
Mean	1.3604	1.3416
Std	0.2036	0.2260

Fig. 18. Pile 2: analysis of the longest dimension and aspect ratio.

denoising remains an active and unsolved research challenge, with no universally accepted parameterization standards analogous to those established for RGB image processing. Optimal filter parameters are inherently dependent on scanner characteristics, stand-off distance, and surface properties, making device-specific benchmarks difficult to generalize (Casajus et al., 2019; Rakotosaona et al., 2020). As noted by

Pile 3

Angularity	Sphericity
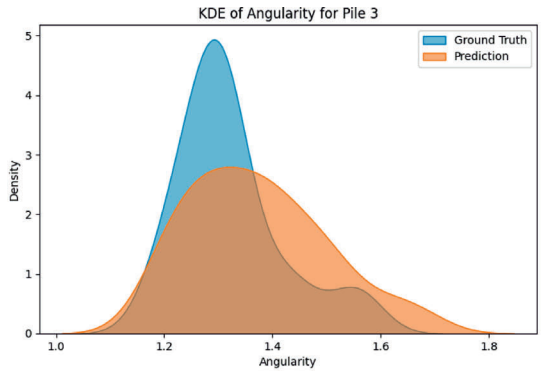	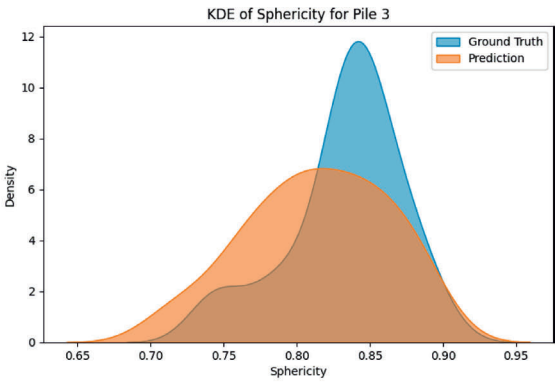
Wasserstein Distance: 0.0514	Wasserstein Distance: 0.0196
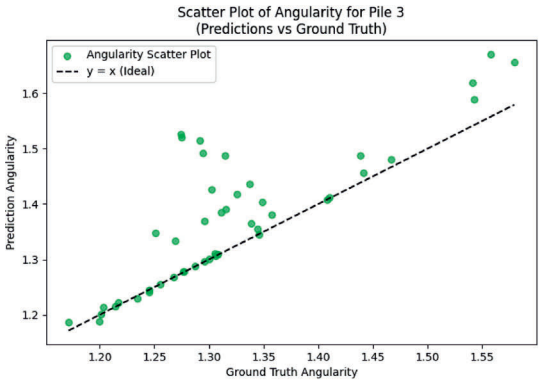	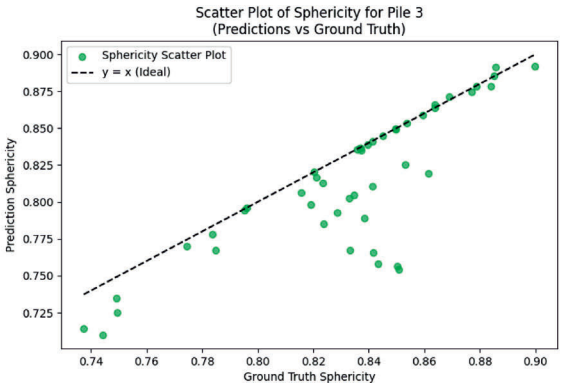
MAPE = 3.87%	*MAPE* = 2.37%

	Ground Truth	Prediction
Mean	1.3216	1.3721
Std	0.0961	0.1247

	Ground Truth	Prediction
Mean	0.8327	0.8135
Std	0.0381	0.0479

Fig. 19. Pile 3: analysis of angularity and sphericity.

Berger et al. (2017), surface reconstruction methods represent a more principled long-term solution to noisy point cloud data than filtering approaches, as they address the underlying geometric representation rather than simply removing outliers. Furthermore, applying more accurate scanners with less noise can increase the accuracy of the data. Occlusion and particle overlap are intrinsic challenges in a rock pile study, as they can affect the accuracy of key metrics like the aspect ratio. A potential solution to this problem could be the automatic

Pile 3

Longest Dimension

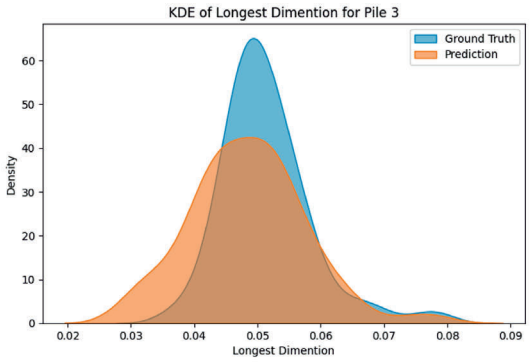

Wasserstein Distance: 0.0030

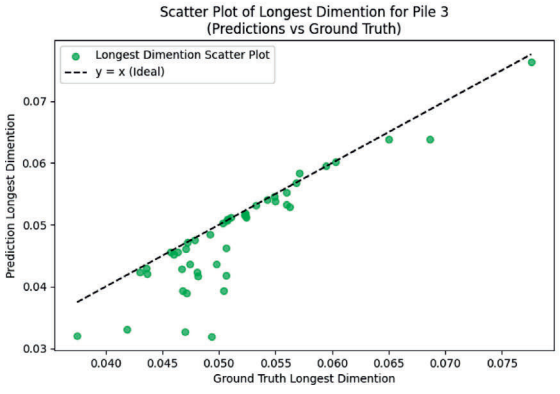

MAPE = 6.21%

	Ground Truth	Prediction
Mean	0.0514	0.0484
Std	0.0070	0.0088

Aspect Ratio

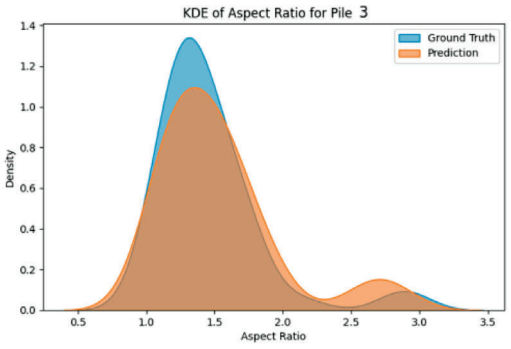

Wasserstein Distance: 0.0866

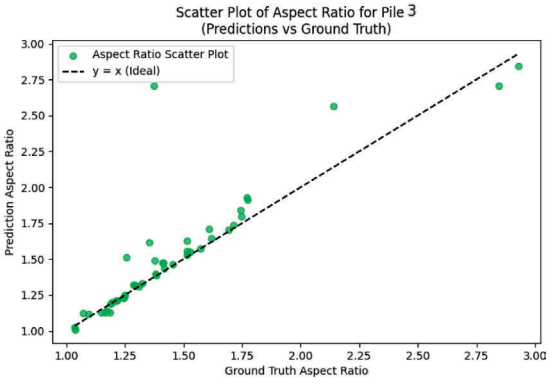

MAPE = 5.80%

	Ground Truth	Prediction
Mean	1.4568	1.5247
Std	0.3813	0.4336

Fig. 20. Pile 3: analysis of the longest dimension and aspect ratio.

exclusion of these occluded particles from the statistical shape/size analysis. However, for a model to automatically identify and exclude occluded rocks, a new dataset with specific 'exposed' and 'occluded' labeling would be required. Looking to the future, Generative AI may offer an alternative solution by filling in the missing data from occluded or partially scanned particles, thus ensuring a more complete analysis.

Additionally, not only does LiDAR-based scanning offer robustness against light, but also the availability of portable and drone-based

LiDAR scanners simplifies data collection and enhances worker safety. However, the technology's deployment in large-scale operations requires further exploration in terms of cost-effectiveness and data processing efficiency. The computational requirements for operational deployment are modest and compatible with standard mining industry hardware. Using a mid-range workstation (NVIDIA RTX 3070 GPU, Intel i7–12700F CPU, 32 GB RAM - approximate cost ~$2500 USD), inference time ranges from 1 s for sparse point clouds to 30 s for dense, complex scenes. Compared to existing image-based systems such as WipFrag and Split Desktop, which require extensive manual editing and post-processing (often taking minutes to hours per analysis depending on image quality and pile complexity), our automated approach offers comparable or faster processing times without manual intervention.

The practical implications of shape prediction errors vary across mining operations. For equipment wear assessment, Ou and Chen (2023) demonstrated that angular particles cause substantially higher crusher liner wear compared to rounded particles. Our Angularity *MAPE* of 3.87–12.37% provides useful guidance for comparative wear assessments across fragmentation events, enabling operators to identify when blast designs produce more angular fragments likely to accelerate equipment degradation. For energy consumption modeling, Gan et al. (2019) showed that increases in particle sphericity correlate with increases in breakage energy in drop weight impact tests, establishing that shape affects comminution efficiency. Our Sphericity accuracy (2.37–6.96% *MAPE*) enables comparative energy assessments, helping operations identify fragmentation patterns that may require adjustment of grinding parameters. For material handling design (conveyor systems, bin geometries, flowability predictions), aspect ratio governs packing density and flow behavior; our measurement accuracy (2.71–16.92% *MAPE*) supports engineering decisions where typical design safety factors exceed 20%. Overall, the achieved prediction accuracy is operationally viable for strategic decision-making (circuit design, maintenance planning, blast pattern optimization) and suitable for tactical monitoring (daily production adjustments), providing quantitative shape data previously unavailable from traditional fragmentation monitoring approaches.

Overall, this study underscores the importance of shape analysis in rock fragmentation and applies a novel framework for its integration into mining workflows. By providing a comprehensive understanding of particle morphology, we enable mining operations to optimize material handling, enhance energy efficiency, and improve safety standards. Additionally, by transitioning from traditional 2D approximations to a comprehensive 3D approach utilizing LiDAR and deep learning, we lay the groundwork for more accurate and actionable insights into particle behaviour. Future research should focus on further refining the proposed methodology, validating the model's performance in diverse mining environments, as well as solutions to reduce noise, thus improving sphericity and angularity results, which are highly affected by the presence of noise in LiDAR data.

6. Conclusion

This study has demonstrated the critical importance of particle shape analysis in rock fragmentation, highlighting its profound impact on mining operations, material handling, and mineral processing. While size distribution has traditionally dominated fragmentation studies, this research underscores that shape characteristics are equally, if not more, influential in determining energy consumption, equipment wear, flowability, processing efficiency, and safety. The limitations of current methodologies in quantitatively and efficiently characterizing the three-dimensional (3D) shape of blasted rock fragments have been identified and addressed.

The research combines LiDAR technology with deep learning-based point cloud segmentation to deliver comprehensive and quantitative 3D particle shape analysis. This method overcomes the inherent limitations of 2D image-based techniques (lighting dependency, 2D analysis of the 3D shapes, qualitative shape analysis, and manual feature extraction), offering a quantitative, scalable, and lighting-independent solution. Validation across three geologically distinct rock piles -blasted limestone, rounded river pebbles, and crushed copper ore- demonstrated that the model achieves shape factor prediction accuracy ranging from 2% to 16% *MAPE* across sphericity, angularity, aspect ratio, and longest dimension measurements. The model's ability to differentiate shape attributes was demonstrated across three different rock piles: blasted rocks, river pebbles, and crushed ore. However, challenges were observed in the sensitivity of sphericity and angularity to the presence of noise in the data.

The successful deployment of this technique marks a considerable stride in mining, providing new insights into particle behavior. By incorporating shape analysis alongside size distribution, mining operations can optimize energy consumption, improve material transport efficiency, reduce maintenance costs, and increase safety. For practical implementation, the method requires only mid-range computing hardware (~$2500 USD) with processing times of a few seconds to a few minutes per scene, making it operationally feasible for real-time fragmentation monitoring in both surface and underground mining environments. The next steps involve model refinement, particularly in addressing the challenges of noise effect on angularity and sphericity, as well as propagating error in aspect ratio predictions, and validating model performance across diverse real-world mining conditions.

CRediT authorship contribution statement

Faramarzi H Mojgan: Writing – original draft, Visualization, Validation, Software, Methodology, Investigation, Formal analysis, Data curation, Conceptualization. **Kamran Esmaeili:** Writing – review & editing, Validation, Supervision, Resources, Project administration, Methodology, Funding acquisition, Conceptualization.

Declaration of Competing Interest

The authors declare that they have no known competing financial interests or personal relationships that could have appeared to influence the work reported in this paper.

Acknowledgment

The authors would like to acknowledge Weir Group and the Natural Science and Engineering Research Council of Canada (NSERC), grant no. ALLRP 561062–20 for their financial support.

References

Ali, U., Kikumoto, M., Ciantia, M., Cui, Y., Previtali, M., 2023. Systematic effect of particle roundness/angularity on macro- and microscopic behavior of granular materials. Granul. Matter 25, 1–16. https://doi.org/10.1007/S10035-023-01341-Y/FIGURES/19

Bamford, T., Esmaeili, K., Schoellig, A.P., 2021. A deep learning approach for rock fragmentation analysis. Int. J. Rock. Mech. Min. Sci. 145, 104839. https://doi.org/10.1016/J.IJRMMS.2021.104839

Bamford, T., Medinac, F., Esmaeili, K., 2020. Continuous monitoring and improvement of the blasting process in open pit mines using unmanned aerial vehicle techniques. Remote Sens (Basel) 12 (17), 2801. https://doi.org/10.3390/rs12172801

Berger, M., Tagliasacchi, A., Seversky, L.M., Alliez, P., Guennebaud, G., Levine, J.A., et al., 2017. A Survey of Surface Reconstruction from Point Clouds. Comput. Graph. Forum. 36, 301–329. https://doi.org/10.1111/cgf.12802

Blender Development Team. Blender. Blender V 34 2022.

Casajus, P.H., Ritschel, T., Ropinski, T., 2019. Total denoising: unsupervised learning of 3D point cloud cleaning. Proceedings of the IEEE International Conference on Computer Vision. 52-60. https://doi.org/10.1109/ICCV.2019.00014

Cleary, P.W., Owen, P., 2019. Effect of particle shape on structure of the charge and nature of energy utilisation in a SAG mill. Min. Eng. 132, 48–68. https://doi.org/10.1016/J.MINENG.2018.12.006

Dai, A., Chang, A.X., Savva, M., Halber, M., Funkhouser, T., Nießner, M., 2017. ScanNet: richly-annotated 3D reconstructions of indoor scenes. Proceedings - 30th IEEE Conference on Computer Vision and Pattern Recognition. CVPR, 2432–2443. https://doi.org/10.1109/CVPR.2017.261

Danjo, K., Kinoshita, K., Kitagawa, K., Iida, K., Sunada, H., Otsuka, A., 1989. Effect of particle shape on the compaction and flow properties of powders. Chem. Pharm. Bull. (Tokyo) 37, 3070–3073. https://doi.org/10.1248/CPB.37.3070

Elmsahli, H.S., Sinka, I.C., 2021. A discrete element study of the effect of particle shape on packing density of fine and cohesive powders. Comput. Part Mech. 8, 183–200. https://doi.org/10.1007/S40571-020-00322-9/FIGURES/16

Faramarzi, H.M., Esmaeili, K., 2025. 3D rock fragmentation analysis using lidar, based on point cloud deep learning segmentation and synthetic data. Powder Technol 456, 120861. https://doi.org/10.1016/J.POWTEC.2025.120861

Feng, R., Bernhardt-Barry, M.L., 2025. Exploring shape quantification of granular particles with a wide range of sizes: a comprehensive framework. Geod. AI 4, 100025. https://doi.org/10.1016/j.geoai.2025.100025

Firouzabadi, M., Esmaeili, K., Rashkolia, G.S., Asadi, M., 2023. A discrete element modelling of gravity flow in sublevel caving considering the shape and size distribution of particles. Int J. Min. Reclam. Environ. 37, 225–276. https://doi.org/10.1080/17480930.2023.2168870

Gan, D., Gao, F., Zhang, Y., Zhang, J., Niu, F., Gan, Z., 2019. Effects of the shape and size of irregular particles on specific breakage energy under drop weight impact. Shock Vib. 2019 (1), 2318571. https://doi.org/10.1155/2019/2318571

Govender, N., Rajamani, R., Wilke, D.N., Wu, C.Y., Khinast, J., Glasser, B.J., 2018. Effect of particle shape in grinding mills using a GPU based DEM code. Min. Eng. 129, 71–84. https://doi.org/10.1016/j.mineng.2018.09.019

Guo, Q., Wang, Y., Yang, S., Xiang, Z., 2022. A method of blasted rock image segmentation based on improved watershed algorithm. Sci. Rep. 12, 7143. https://doi.org/10.1038/s41598-022-11351-0

Ikeda, H., Sato, T., Yoshino, K., Toriya, H., Jang, H., Adachi, T., Kitahara, I., Kawamura, Y., 2023. Deep learning-based estimation of muckpile fragmentation using simulated 3D point cloud data. Appl. Sci. 13, 10985. https://doi.org/10.3390/APP131910985

Koh, P.T.L., Hao, F.P., Smith, L.K., Chau, T.T., Bruckard, W.J., 2009. The effect of particle shape and hydrophobicity in flotation. Int J. Min. Process 93, 128–134. https://doi.org/10.1016/J.MINPRO.2009.07.007

Li, R., Lu, W., Chen, M., Wang, G., Xia, W., Yan, P., 2021. Quantitative analysis of shapes and specific surface area of blasted fragments using image analysis and three-dimensional laser scanning. Int. J. Rock. Mech. & Min. Sci. 141, 1365–1609. https://doi.org/10.1016/j.ijrmms.2021.104710

Li, R., Zhu, P., Li, S., Ding, C., Lu, W., Liu, Y., 2023. Fractal behavior of size distribution and specific surface area of blasting fragments. Appl. Sci. 13 (21), 11832. https://doi.org/10.3390/app132111832

Ma, G., Wang, Y., Zhou, H., Lu, X., Zhou, W., 2022. Morphology characteristics of the fragments produced by rock grain crushing. Int. J. Geomech. 22 (4), 04022020. https://doi.org/10.1061/(asce)gm.1943-5622.0002329

Ou, T., Chen, W., 2023. Modelling of gyratory crusher liner wear using a digital wireless sensor. Sensors 23 (21), 8818. https://doi.org/10.3390/S23218818

Ouchterlony, F., 2003. Influence of blasting on the size distribution and properties of muckpile fragments: a state-of-the-art review. MinFo project P2000-10: Energioptimering vid nedbrytning / Energy optimisation in comminution.

Pereira, L., Schach, E., Tolosana-Delgado, R., Frenzel, M., 2023. All about particles: modelling ore behaviour in mineral processing. Elements 19, 359–364. https://doi.org/10.2138/GSELEMENTS.19.6.359

Rakotosaona, M.J., La Barbera, V., Guerrero, P., Mitra, N.J., Ovsjanikov, M., 2020. PointCleanNet: learning to denoise and remove outliers from dense point clouds. Comput. Graph. Forum. 39, 185–203. https://doi.org/10.1111/cgf.13753

Reitmann, S., Neumann, L., Jung, B., 2021. Blainder—a blender ai add-on for generation of semantically labeled depth-sensing data. Sensors. 21 (6), 2144. https://doi.org/10.3390/s21062144

Schenk, F., Tscharf, A., Mayer, G., Fraundorfer, F., 2019. Automatic muck pile characterization from UAV images. ISPRS Ann. Photogramm. Remote Sens. Spat. Inf. Sci. IV-2-W5, 163–170. https://doi.org/10.5194/ISPRS-ANNALS-IV-2-W5-163-2019

Tang, C., Yang, Y.-C., Liu, P.-Z., Kim, Y.-J., 2021. Prediction of abrasive and impact wear due to multi-shaped particles in a centrifugal pump via CFD-DEM coupling. methodEnergies 14 (9), 2391. https://doi.org/10.3390/EN14092391

Taylor, M.A., 2002. Quantitative measures for shape and size of particles. Powder Technol. 124, 94–100. https://doi.org/10.1016/S0032-5910(01)00476-4

Ulusoy, U., 2023. A review of particle shape effects on material properties for various engineering applications: from macro to nanoscale. Minerals 13 (1), 91. https://doi.org/10.3390/min13010091

Unland, G., Al-Khasawneh, Y., 2009. The influence of particle shape on parameters of impact crushing. Min. Eng. 22 (3), 220–228. https://doi.org/10.1016/j.mineng.2008.08.008

Vu, T., Kim, K., Luu, T.M., Nguyen, T., Yoo, C.D., 2022. SoftGroup for 3D Instance Segmentation on Point Clouds. Proceedings of the IEEE Computer Society Conference on Computer Vision and Pattern Recognition. 2698-2707. https://doi.org/10.1109/CVPR52688.2022.00273

Wang, L., Jing, H., Yu, J., Liu, X., 2022. Impact of particle shape, size, and size distribution on gravity flow behaviour of broken ore in sublevel caving. Minerals. 12 (10), 1183. https://doi.org/10.3390/min12101183

Wang, W., Li, Q., Xiao, C., Zhang, D., Miao, L., Wang, L., 2021. An improved boundary-aware U-Net for ore image semantic segmentation. Sensors 21 (8), 2615. https://doi.org/10.3390/S21082615

Wang, Y., Tu, W., Li, H., 2021. Fragmentation calculation method for blast muck piles in open-pit copper mines based on three-dimensional laser point cloud data. Int. J. Appl. Earth Obs. Geoinf. 100, 102338. https://doi.org/10.1016/j.jag.2021.102338

Wills, B.A., Finch, J.A., 2015. Wills' mineral processing technology: an introduction to the practical aspects of ore treatment and mineral recovery. Elsevier Inc. https://doi.org/10.1016/C2010-0-65478-2

Wills, B.A., Napier-munn, T., 2006. Mineral Processing Technology An Introduction to the Practical Aspects of Ore Treatment and Mineral Recovery. October 2006:444.

Xia, W., 2017. Role of particle shape in the floatability of mineral particle: an overview of recent advances. Powder Technol. 317, 104–116. https://doi.org/10.1016/J.POWTEC.2017.04.050

Yang, X., Ren, T., Tan, L., 2020. Size distribution measurement of coal fragments using digital imaging processing. Meas. (Lond.) 160, 107867. https://doi.org/10.1016/j.measurement.2020.107867

Yang, Z., He, B., Liu, Y., Wang, D., Zhu, G., 2021. Classification of rock fragments produced by tunnel boring machine using convolutional neural networks. Autom. Constr. 125, 103612. https://doi.org/10.1016/J.AUTCON.2021.103612

Zardari, M.A., 2011. Stability of Tailings Dams Focus on Numerical Modelling. Luleå University of Technology.

Zhao, J., Li, D., Yu, Y., Zhao, Junjie, Li, Diyuan, Yu, Yisong, 2024. Identification of rock fragments after blasting by using deep learning-based segment anything model. Minerals. 14 (7), 654. https://doi.org/10.3390/MIN14070654

Zyuzin, V., Ronkin, M., Porshnev, S., Kalmykov, A., 2021. Automatic asbestos control using deep learning based computer vision system. Appl. Sci. 11 (22), 10532. https://doi.org/10.3390/APP112210532